NASA TECHNICAL NOTE

NASA TN D-6841

EFFECT OF EDDY DIFFUSIVITY ON WIND-DRIVEN CURRENTS IN A TWO-LAYER STRATIFIED LAKE

by Richard T. Gedney, W. Lick, and Frank B. Molls

Lewis Research Center
Cleveland, Ohio 44135

NATIONAL AERONAUTICS AND SPACE ADMINISTRATION • WASHINGTON, D. C. • JUNE 1972

1. Report No. NASA TN D-6841	2. Government Accession No.
3. Recipient's Catalog No.	
4. Title and Subtitle EFFECT OF EDDY DIFFUSIVITY ON WIND-DRIVEN CURRENTS IN A TWO-LAYER STRATIFIED LAKE	5. Report Date June 1972
	6. Performing Organization Code
7. Author(s) Richard T. Gedney, Lewis Research Center; W. Lick, Case Western Reserve University; and Frank B. Molls, Lewis Research Center	8. Performing Organization Report No. E-6776
9. Performing Organization Name and Address Lewis Research Center National Aeronautics and Space Administration Cleveland, Ohio 44135	10. Work Unit No. 136-13
	11. Contract or Grant No.
12. Sponsoring Agency Name and Address National Aeronautics and Space Administration Washington, D.C. 20546	13. Type of Report and Period Covered Technical Note
	14. Sponsoring Agency Code
15. Supplementary Notes	

16. Abstract

The steady-state wind-driven circulation is numerically calculated in a rectangular stratified lake. The lake is composed of two layers having uniform but unequal densities and eddy diffusivities. The position of thermocline and the three-dimensional velocities in both layers are calculated using the shallow lake equations of P. Welander. The results show that, as the eddy diffusivity in the hypolimnion is increased, the thermocline tilt and hypolimnetic velocities increase. The effect of the other variables such as wind stress, density, basin length, and mean thermocline depth are also shown.

17. Key Words (Suggested by Author(s)) Three-dimensional flow Stratified lake currents Eddy diffusivity for lakes Incompressible turbulent flow	18. Distribution Statement Unclassified - unlimited		
19. Security Classif. (of this report) Unclassified	20. Security Classif. (of this page) Unclassified	21. No. of Pages 38	22. Price* $3.00

* For sale by the National Technical Information Service, Springfield, Virginia 22151

EFFECT OF EDDY DIFFUSIVITY ON WIND-DRIVEN CURRENTS IN A TWO-LAYER STRATIFIED LAKE

by Richard T. Gedney, W. Lick,* and Frank B. Molls

Lewis Research Center

SUMMARY

The steady-state wind-driven circulation is numerically calculated in a rectangular stratified lake. The lake is composed of two layers (an upper, warmer layer termed the epilimnion and a lower, cooler layer termed the hypolimnion) having uniform but unequal densities and eddy diffusivities. The position of the interface between the two layers (the thermocline) and the three-dimensional velocities in both layers are calculated using the shallow lake equations of P. Welander. Continuity of velocity and shear stress are maintained across the thermocline.

Because the values of the eddy diffusivities in the layers are not well known, results for hypolimnetic diffusivities from 1.05 to 16.8 square centimeters per second and epilimnetic diffusivities from 16.8 to 67.2 square centimeters per second are given. In the examples calculated the length of the lake is of order 100 kilometers, the wind velocity is 5.2 meters per second, and the temperature difference between the epilimnion and hypolimnion is 18° C. The results show that, as the hypolimnetic diffusivity is increased, the thermocline tilt and hypolimnetic velocities increase. The effect of the other variables (wind stress, density, basin length, and mean thermocline depth) are easily discerned from the analysis. It is shown that the solution for a rectangular basin is not strongly dependent upon the length to width ratio of the basin. Therefore, most of the results are given for a square basin.

INTRODUCTION

As part of the present day analysis of the effects of pollution on large lakes, models are being developed which will attempt to predict the lake's chemical and biological

*Professor of Geophysics and Engineering, Case Western Reserve University, Cleveland, Ohio. Professor Lick's work was supported by the National Science Foundation.

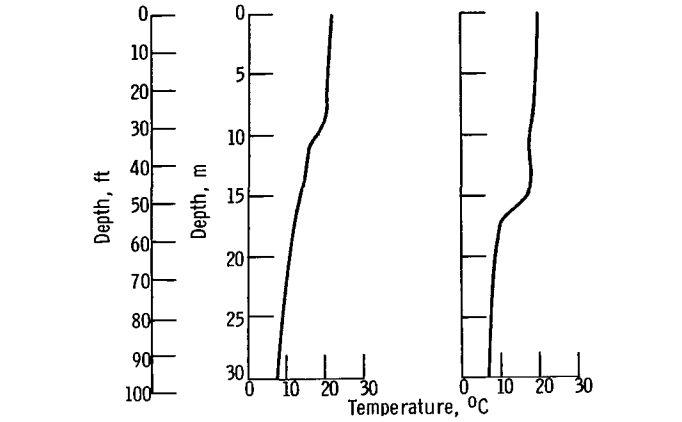

(a) Average temperature profile in Cayuga Lake for period between August 14th and August 20th, 1968. (Data taken from ref. 1.)

(b) Average temperature profile in Cayuga Lake for period between September 25th and October 1st, 1968. (Data taken from ref. 1.)

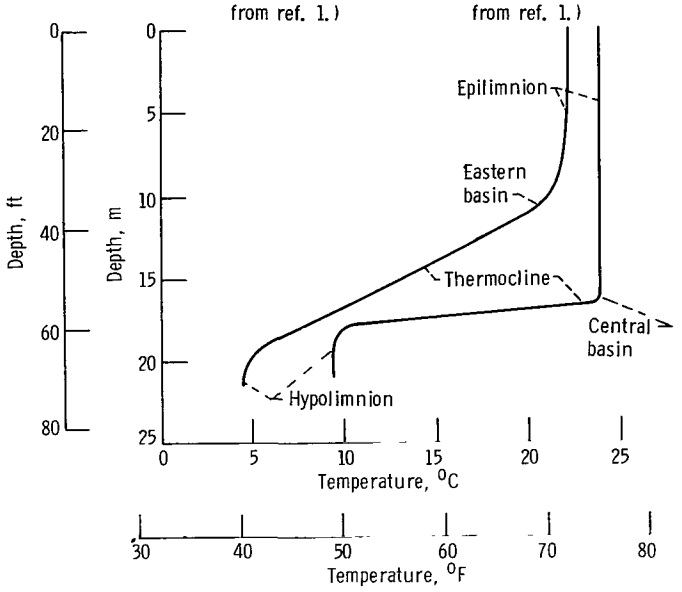

(c) Typical summer temperature profile in Lake Erie. (Taken from ref. 11.)

Figure 1. - Typical stratified lake temperature profiles.

changes as a function of the pollution added to the system. Development of these models requires knowledge of the currents during the summer when the lake water has a very definite vertical temperature stratification.

A typical thermally stratified lake, such as the one described in figure 1, can usually be divided into three zones: the upper region called the epilimnion, the middle region, where the temperature gradient is steepest, called the metalimnion, and the bottom region called the hypolimnion. The thermocline is defined as the surface of

maximum rate of decrease in temperature. As is well known, the stable temperature gradient shown in figure 1 suppresses turbulence generated by the wind shear in the surface layers of the lake so that near the thermocline the turbulence intensity is greatly reduced from that encountered at the surface. This is well illustrated by the plot (fig. 2) of eddy diffusivity for heat ν_H as calculated by Sundaram, Esterbrook, Piech, and Rudinger (ref. 1) from the data which was used to construct the figure 1(a) temperature curve. In general, it has been found that the eddy diffusivities for heat and momentum under arbitrary thermal stratification conditions are a function of a stability parameter.

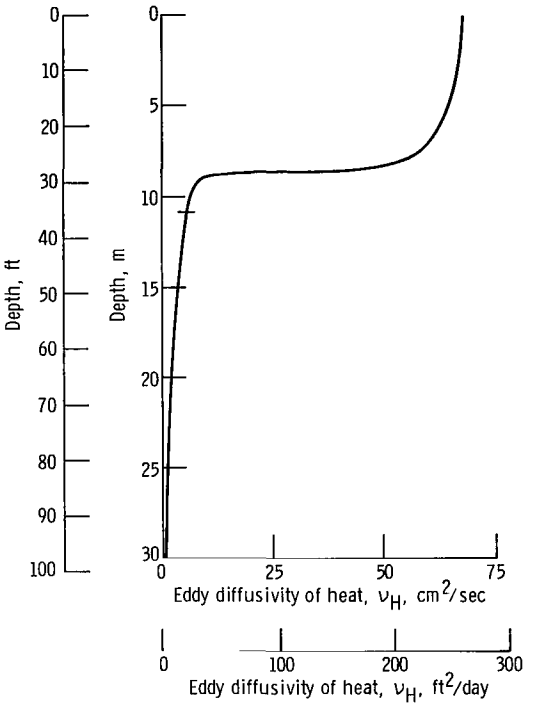

Figure 2. - Calculation of vertical eddy diffusivity in Cayuga Lake for period between August 14th and August 27th, 1968. (Data taken from ref. 1.)

One of the more commonly used forms of the stability parameter is the Richardson number Ri which is defined as

$$\mathrm{Ri} = \alpha_v g \frac{(\partial T/\partial Z)}{(\partial U/\partial Z)^2}$$

where α_v is the coefficient of volumetric expansion of water, g is the acceleration due to gravity, U is the horizontal velocity, Z is the vertical coordinate increasing upward,

and T is the temperature. Under conditions of neutral stability, Ri = 0, the eddy diffusivity of momentum and heat are generally assumed to be the same, that is, $\nu_M = \nu_H$. The dependence of ν_M and ν_H on Ri has to date only been determined empirically. Because this empiricism has not been well established for ν_M, the exact dependence of the turbulent Prandtl number ν_M/ν_H, on stability is a point of some controversy. It is generally believed for lake models (Hutchinson, ref. 2) that ν_M/ν_H increases with increasing Ri. In any event, in the upper part of the epilimnion where the temperature gradient is small and as a result Ri is small, the ratio ν_M/ν_H will be close to 1.0. For the balance of the lake, ν_M should qualitatively have a similar profile as that shown in figure 2.

The plots in figures 1 and 2 are based on average temperatures over a 1-week period during which time-dependent seiche currents existed. The internal waves associated with the seiche currents generate turbulence which diffuses the sharp temperature gradient in the neighborhood of the thermocline. During a period of steady winds, the temperature gradients in the hypolimnion and epilimnion and the thickness of the metalimnion are generally much less than shown in the figures.

The results just discussed for the temperature and eddy diffusivities suggest that the lake stratification may be modeled by considering the lake to be made up of two homogeneous layers each with different densities and eddy diffusivities with the interface between the two layers being located at the thermocline. At the interface, velocity and shear stress should be continuous. It is felt that this two-layer model which will be analyzed here will give a qualitative understanding of the dependence of stratified lake currents on the value of the governing parameters in the epilimnion and hypolimnion. A model in which the density and eddy diffusivities vary continuously with the vertical coordinate can be analyzed in the future when the dependence of ν_M on stability is better established. Since the two-layer model is most applicable under the condition of steady winds, it will only be solved assuming the wind stress is independent of time.

Welander (ref. 3) and others have studied a two-layered model for the oceans which includes the Ekman dynamics assumption that the shear stress at the thermocline and the lake bottom are proportional to the geostrophic (inviscid) velocities in either the hypolimnion or epilimnion. In addition, at one point in their analyses the velocity in the hypolimnion is assumed zero which allows the transport equation for the epilimnion to be uncoupled from the one for the hypolimnion. Others such as Hamblin (ref. 4) have used this approach in the Great Lakes. In fresh water lakes, the thickness of the friction layer generated by the wind is of the order of or greater than the average thickness of the epilimnion; and there is no geostrophic (inviscid) flow in the interior of the epilimnion. Therefore Ekman dynamics cannot be used. In this analysis the shallow lake type equations originally derived by Welander (ref. 5) and shown by Gedney and Lick (ref. 6) to yield good quantitative results for Lake Erie during uniform temperature conditions

(no stratification) will be used. We also make no assumption pertaining to the hypolimnion velocity magnitude and will determine the effect of the hypolimnion eddy diffusivity magnitude as well as the other governing parameters on the two-layer solution.

Since the value of the eddy diffusivities are not well established, a wide range of values should be investigated. In order to accomplish this, a numerical solution of the complete two-layer equations was performed. This numerical solution is presented here. In a paper to be published an asymptotic expansion solution for the case when the hypolimnion eddy diffusivity is small will be given.

Lee (ref. 7) performed a numerical solution for a two-layer lake using the shallow lake type equations. Lee's formulation and numerical procedure is different than the one used here and, because it allows the thermocline to intercept a variable bottom, is much more complex. His reported results, which are for one set of eddy diffusivities at wind shear stresses that may be too small, do not demonstrate the effect of eddy diffusivity. We consider here a parameter study over a wider range to demonstrate the effect of eddy diffusivity. In addition we are able to check our numerical results with analytical ones in the limit of small hypolimnion eddy diffusivities.

SYMBOLS

A_1	coefficient defined by eq. (8)
A_2	coefficient defined by eq. (9)
a_1	$\omega\alpha_1\xi$
a_2	$\omega\alpha_2(h + \xi)$
C_K	coefficient defined in appendix A
$D_1, D_2, D_{1\xi}, D_{2\xi}$, DSCK	coefficients defined in appendix A
d_1	epilimnion friction depth
d_2	hypolimnion friction depth
$E_1, E_2, E_{1\xi}, E_{2\xi}$	coefficients defined in appendix A
$F_1, F_2, F_{1\xi}, F_{2\xi}$	coefficients defined in appendix A
f_c	Coriolis parameter

G_{ij}	coefficients defined in appendix B where i = 1, 2, . . ., 10 and j = 1, 2
g	acceleration of gravity
H	dimensional lake depth
h	nondimensional lake depth
K, K_h	coefficients defined in appendix A
L	reference length of lake
M	number of x grid points
M_{1T}	$M_{1x} + iM_{1y}$, epilimnion volume transport
M_{2T}	$M_{2x} + iM_{2y}$, hypolimnion volume transport
$\hat{m}$	unit normal vector to boundary
m_1, m_2	x and y components of $\hat{m}$
N	number of y grid points
$\frac{\partial}{\partial N}$	$\frac{\partial}{\partial X} + i\frac{\partial}{\partial Y}$
$\frac{\partial}{\partial n}$	$\frac{\partial}{\partial x} + i\frac{\partial}{\partial y}$
$\frac{\partial}{\partial n^*}$	$\frac{\partial}{\partial x} - i\frac{\partial}{\partial y}$
P	dimensional pressure
Ri	Richardson number
T	dimensional temperature
U_{ref}	reference dimensional velocity
u, U	velocity in x direction
v, V	velocity in y direction
w, W	velocity in x direction
x, X y, Y z, Z	Cartesian coordinates
α_v	coefficient of volumetric expansion
α_1	$2\pi\xi_{ref}/d_1$

α_2	$2\pi\xi_{ref}/d_2$
β	length to width ratio in a rectangular basin
Γ_1	$u_1 + iv_1$
Γ_2	$u_2 + iv_2$
Δ	mesh spacing
∇^2	$\frac{\partial^2}{\partial x^2} + \frac{\partial^2}{\partial y^2}$
ζ	nondimensional surface displacement
κ_τ	$d_2/d_1\rho_r$
ν_H	eddy diffusivity of heat
ν_M	eddy diffusivity of momentum
ξ	nondimensional thermocline position
ρ	density
$\Delta\rho$	$(\rho_2 - \rho_1)/\rho_1$
ρ_r	ρ_1/ρ_2
τ^w	wind shear stress $\tau_x^w + i\tau_y^w$
ω	$(1 + i)/2$

Subscripts:

h	indicated derivative with respect to h
k	indicates mesh point x location
l	indicates mesh point y location
ref	as in ξ_{ref}
1	epilimnion
2	hypolimnion

Superscripts:

(r)	real part
(i)	imaginary part
n	iteration number
$(\bar{\ })$	indicates dimensional quantity

FORMULATION

Basic Equations and Boundary Conditions

In the present analysis, the lake is considered to be composed of two layers of different density as shown in figure 3. In each layer, the basic approximations are that the water density is constant, the vertical eddy viscosity is independent of position, the pressure is hydrostatic (i.e., it is determined by water column height), and the lateral friction and nonlinear acceleration terms can be neglected. The explanation for the density and eddy diffusivity being considered constant in each layer has already been given in the INTRODUCTION. Gedney (refs. 8 and 9) has shown the other assumptions to be good approximations for the Great Lakes.

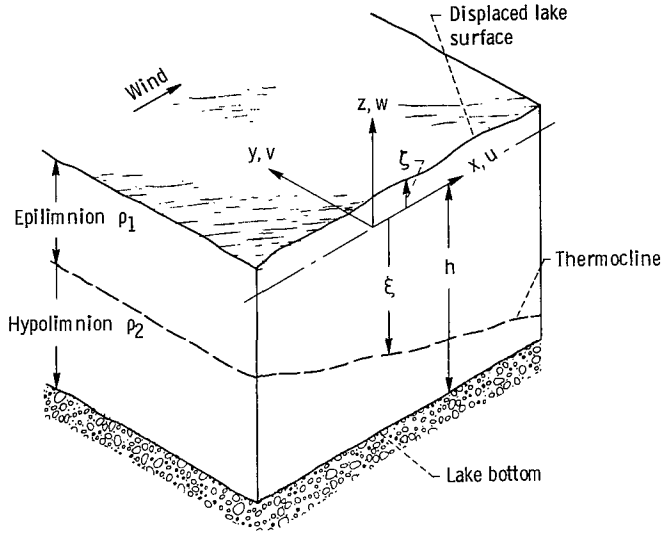

Figure 3. - Cartesian coordinates for stratified lake.

Seiche currents which occur when the wind varies rapidly are very important in stratified lakes but there are periods when the winds are essentially steady. It is during the steady wind period that the temperature gradient at the thermocline is the sharpest and as a result the period when the lake is best approximated by two layers. The properties of the eddy diffusivities are also known best for a steady wind. As a first step, the analysis performed here will assume steady winds.

As is well known, the thermocline position in a stratified lake being acted upon by a steady wind will slowly sink. The rate of deepening has been measured in Cayuga Lake (see ref. 1) to be in the neighborhood of 15 to 30 centimeters per day. This rate is of such magnitude that the time derivative terms in the momentum equations can be ne-

glected and the problem is then "quasi-steady." With the steady wind restriction plus the assumptions stated, the momentum equations and the continuity equation applicable to each layer shown in figure 3 are

$$\frac{\partial U_j}{\partial X} + \frac{\partial V_j}{\partial Y} + \frac{\partial W_j}{\partial Z} = 0 \qquad j = 1,\ 2 \tag{1a}$$

$$\left.\begin{aligned} -f_c V_j &= -\frac{1}{\rho_j}\frac{\partial P_j}{\partial X} + \nu_{Mj}\frac{\partial^2 U_j}{\partial Z^2} \\ +f_c U_j &= -\frac{1}{\rho_j}\frac{\partial P_j}{\partial Y} + \nu_{Mj}\frac{\partial^2 V_j}{\partial Z^2} \end{aligned}\right\} \quad j = 1,\ 2 \tag{2}$$

$$\frac{\partial P_j}{\partial Z} = -\rho_j g \qquad j = 1,\ 2 \tag{3}$$

As shown in figure 3 the Cartesian coordinate system used has X increasing eastward, Y northward, and Z vertically upward with the corresponding velocities being U_j, V_j, and W_j where $j = 1$ indicates the epilimnion and $j = 2$ indicates the hypolimnion. In these equations f_c is the Coriolis parameter, ρ_j is the density, P_j is the pressure, ν_{Mj} is the vertical eddy diffusivity, and g is the acceleration due to gravity. Effects due to the Earth's curvature and to the variation in Coriolis force with position have been neglected since the scales of lakes are much less than the radius of the Earth.

By integrating the hydrostatic equation (3) vertically from the surface of the lake, $Z = \overline{\zeta}$, to an arbitrary point in the epilimnion and from the thermocline, $Z = \overline{\xi}$, to an arbitrary point in the hypolimnion, we obtain the equations for the pressure in the epilimnion and hypolimnion as

$$P_1(X, Y, Z) = P_1\left[\overline{\zeta}(X, Y)\right] - \rho_1 g Z + \rho_1 g\overline{\zeta}(X, Y)$$

$$P_2(X, Y, Z) = P_1\left[\overline{\zeta}(X, Y)\right] - \rho_2 g Z + (\rho_2 - \rho_1) g\overline{\xi}(X, Y) + \rho_1 g\overline{\zeta}(X, Y)$$

In most cases the effects caused by the variation of P_1 at the surface are small so that they can be neglected. Combining these pressure equations with the momentum equations (2) results in

$$\rho_1 \nu_{M1} \frac{\partial^2 \bar{\Gamma}_1}{\partial Z^2} - i\rho_1 f_c \bar{\Gamma}_1 = \rho_1 g \frac{\partial \bar{\zeta}}{\partial N} \tag{4a}$$

$$\rho_2 \nu_{M2} \frac{\partial^2 \bar{\Gamma}_2}{\partial Z^2} - i\rho_2 f_c \bar{\Gamma}_2 = \rho_1 g \left(\Delta\rho \frac{\partial \bar{\xi}}{\partial N} + \frac{\partial \bar{\zeta}}{\partial N} \right) \tag{5a}$$

where

$$\Delta\rho = \frac{\rho_2 - \rho_1}{\rho_1}$$

$$\rho_r = \frac{\rho_1}{\rho_2}$$

$$\bar{\Gamma}_1 = U_1 + iV_1$$

$$\bar{\Gamma}_2 = U_2 + iV_2$$

$$\frac{\partial \bar{\zeta}}{\partial N} = \frac{\partial \bar{\zeta}}{\partial X} + i \frac{\partial \bar{\zeta}}{\partial Y}$$

$$\frac{\partial \bar{\xi}}{\partial N} = \frac{\partial \bar{\xi}}{\partial X} + i \frac{\partial \bar{\xi}}{\partial Y}$$

The aforementioned equations may be made nondimensional by introducing the following variables:

$$\zeta = \frac{\bar{\zeta}}{\zeta_{ref}}, \quad x = \frac{X}{L}, \quad y = \frac{Y}{L}, \quad n = \frac{N}{L}, \quad \Gamma = \frac{\bar{\Gamma}}{U_{ref}}, \quad \xi = \frac{\bar{\xi}}{\xi_{ref}}, \quad z = \frac{Z}{\xi_{ref}},$$

$$w = \frac{L}{\xi_{ref} U_{ref}} W, \quad u = \frac{U}{U_{ref}}, \quad v = \frac{V}{U_{ref}}, \quad \zeta_{ref} = \frac{2\pi L \tau^W_{ref}}{\rho_1 d_1 g}, \quad \xi_{ref} = \frac{\zeta_{ref}}{\Delta\rho},$$

$$U_{ref} = \frac{\pi \tau^w_{ref}}{\rho_1 d_1 f_c}, \qquad d_1 = \pi \sqrt{\frac{2\nu_{M1}}{f_c}}, \qquad d_2 = \pi \sqrt{\frac{2\nu_{M2}}{f_c}}, \qquad \alpha_1 = \frac{2\pi\xi_{ref}}{d_1}, \qquad \alpha_2 = \frac{2\pi\xi_{ref}}{d_2},$$

With these quantities the dimensional equations (1a), (4a), and (5a) become

$$\frac{\partial u_1}{\partial x} + \frac{\partial v_1}{\partial y} + \frac{\partial w_1}{\partial z} = 0 \tag{1b}$$

$$\frac{\partial u_2}{\partial x} + \frac{\partial v_2}{\partial y} + \frac{\partial w_2}{\partial z} = 0 \tag{1c}$$

$$\frac{1}{\alpha_1^2} \frac{\partial^2 \Gamma_1}{\partial z^2} - \frac{i}{2} \Gamma_1 = \frac{\partial \zeta}{\partial n} \tag{4b}$$

$$\frac{1}{\alpha_2^2} \frac{\partial^2 \Gamma_2}{\partial z^2} - \frac{i}{2} \Gamma_2 = \rho_r \left(\frac{\partial \xi}{\partial n} + \frac{\partial \zeta}{\partial n} \right) \tag{5b}$$

where the continuity equation (1a) has been written for both the hypolimnion and epilimnion.

This system of equations must now be solved subject to the following boundary conditions:

$$\left.\begin{aligned} \tau^w = \tau^w_x + i\tau^w_y = \frac{1}{\alpha_1} \frac{\partial \Gamma_1}{\partial z} \quad &\text{at } z = 0 \\ \Gamma_2 = w_2 = 0 \quad &\text{at } z = -h(x,y) \\ \left.\begin{aligned} \Gamma_1 &= \Gamma_2 \\ \frac{\partial \Gamma_1}{\partial z} &= \frac{d_2^2}{d_1^2} \frac{1}{\rho_r} \frac{\partial \Gamma_2}{\partial z} \end{aligned}\right\} \quad &\text{at } z = \xi(x,y) \end{aligned}\right\} \tag{6}$$

$$\left.\begin{aligned} w_1 &= 0 \quad \text{at} \quad z = 0 \\ w_1 &= u_1 \frac{\partial \xi}{\partial x} + v_1 \frac{\partial \xi}{\partial y} \\ w_2 &= u_2 \frac{\partial \xi}{\partial x} + v_2 \frac{\partial \xi}{\partial y} \end{aligned}\right\} \quad \text{at} \quad z = \xi(x, y) \tag{7}$$

where h is the depth of the lake. The w_1 and w_2 velocity boundary conditions at $z = \xi(x, y)$ are such that there is no flow normal to the thermocline. For strong enough winds the thermocline may intersect the surface of the water with an upwelling of cold bottom waters resulting. In this case, which will not be considered, there would be a velocity normal to the thermocline which would reflect the volume decrease in the hypolimnion due to the upwelling.

In this analysis all surface boundary conditions are applied at $z = 0$ (no wind position) instead of at $z = \zeta$. For the cases to be calculated here it can readily be shown (see refs. 8 and 9 for error estimates for shallow Lake Erie) that evaluating the surface boundary conditions at $z = 0$ induces an error of a few percent which is only local in extent.

Governing Equations for the Surface Displacement and the Thermocline

Equations (4b) and (5b) subject to the boundary conditions (6) can be solved for the horizontal velocities in the hypolimnion and epilimnion as functions of the surface displacement ζ, the thermocline position ξ, the lake depth h, and the wind stress τ^w. The resulting solutions are

$$\Gamma_1 = A_1 e^{\omega\alpha_1(\xi - z)} + A_1 e^{\omega\alpha_1(\xi + z)} + \frac{\tau^w}{\omega} e^{\omega\alpha_1 z} + 2i \frac{\partial \zeta}{\partial n} \qquad \xi \le z \le 0 \tag{8}$$

$$\Gamma_2 = \left[A_2 - 2i\rho_r\left(\frac{\partial \zeta}{\partial n} + \frac{\partial \xi}{\partial n}\right)\right] e^{\omega\alpha_2(h+z)} - A_2 e^{-\omega\alpha_2(h+z)} + 2i\rho_r\left(\frac{\partial \zeta}{\partial n} + \frac{\partial \xi}{\partial n}\right) \qquad -h \le z \le \xi \tag{9}$$

where

$$A_1 = \frac{2i\rho_r \kappa_\tau}{K}\left(\frac{\partial\zeta}{\partial n} + \frac{\partial\xi}{\partial n}\right)\left(1 + e^{-2a_2} - 2e^{-a_2}\right) - \frac{2i\kappa_\tau}{K}\left(\frac{\partial\zeta}{\partial n}\right)\left(1 + e^{-2a_2}\right)$$

$$+ \frac{\tau^w}{\omega}\frac{e^{a_1}}{K}\left[\left(1 - e^{-2a_2}\right) - \kappa_\tau\left(1 + e^{-2a_2}\right)\right]$$

$$A_2 = \frac{2\tau^w}{\omega}\frac{e^{a_1}e^{-a_2}}{K} - \frac{2i\rho_r}{K}\left[\left(e^{2a_1} - 1\right)\left(1 - e^{-a_2}\right) - \kappa_\tau\left(e^{2a_1} + 1\right)\right]\left(\frac{\partial\zeta}{\partial n} + \frac{\partial\xi}{\partial n}\right)$$

$$- \frac{2i}{K}e^{-a_2}\left(e^{2a_1} - 1\right)\left(\frac{\partial\zeta}{\partial n}\right)$$

$$a_1 = \omega\alpha_1\xi$$

$$a_2 = \omega\alpha_2(h + \xi)$$

$$\omega = \frac{1 + i}{2}$$

$$\kappa_\tau = \frac{d_2}{d_1\rho_r}$$

$$K = \kappa_\tau\left(1 + e^{-2a_2}\right)\left(1 + e^{2a_1}\right) - \left(1 - e^{-2a_2}\right)\left(e^{2a_1} - 1\right)$$

The w_1 and w_2 velocities can readily be determined, respectively, by combining equations (1b) and (8) and equations (1c) and (9).

The velocity equations (8) and (9) and the continuity equations (1b) and (1c) can be integrated vertically to give

$$M_{1T} = M_{1x} + iM_{1y} = \int_\xi^0 \alpha_1\Gamma_1\, dz = D_1\tau^w + E_1\frac{\partial\zeta}{\partial n} + F_1\frac{\partial\xi}{\partial n} \tag{10}$$

$$M_{2T} = M_{2x} + iM_{2y} = \int_h^\xi \alpha_2\Gamma_2\, dz = D_2\tau^w + E_2\frac{\partial\zeta}{\partial n} + F_2\frac{\partial\xi}{\partial n} \tag{11}$$

$$\frac{\partial M_{1x}}{\partial x} + \frac{\partial M_{1y}}{\partial y} = 0 \tag{12a}$$

$$\frac{\partial M_{2x}}{\partial x} + \frac{\partial M_{2y}}{\partial y} = 0 \tag{13a}$$

where the coefficients D_1, E_1, F_1, D_2, E_2, and F_2 are functions of the local depth $h(x, y)$ and the thermocline position $\xi(x, y)$, and are given in appendix A. The quantities M_{1T} and M_{2T} are respectively the volume transport in the epilimnion and hypolimnion.

Equations (10) to (13a) can be combined to obtain two coupled equations for ζ and ξ. Equations (12a) and (13a) are equivalent to

$$\text{Real}\left(\frac{\partial M_{1T}}{\partial n^*}\right) = 0 \tag{12b}$$

$$\text{Real}\left(\frac{\partial M_{2T}}{\partial n^*}\right) = 0 \tag{13b}$$

where

$$\frac{\partial}{\partial n^*} = \frac{\partial}{\partial x} - i\frac{\partial}{\partial y}$$

By substituting equations (10) and (11) into equations (12b) and (13b) we find the two equations for ζ and ξ are

$$\begin{aligned} F_j^{(r)}\nabla^2\xi + E_j^{(r)}\nabla^2\zeta &+ \left[E_{j\xi}^{(r)}\frac{\partial\zeta}{\partial x} - E_{j\xi}^{(i)}\frac{\partial\zeta}{\partial y} + F_{jh}^{(r)}\frac{\partial h}{\partial x} + F_{jh}^{(i)}\frac{\partial h}{\partial y} + F_{j\xi}^{(r)}\frac{\partial\xi}{\partial x} + \tau_x^w D_{j\xi}^{(r)} - \tau_y^w D_{j\xi}^{(i)}\right]\frac{\partial\xi}{\partial x} \\ &+ \left[E_{j\xi}^{(i)}\frac{\partial\zeta}{\partial x} + E_{j\xi}^{(r)}\frac{\partial\zeta}{\partial y} - F_{jh}^{(i)}\frac{\partial h}{\partial x} + F_{jh}^{(r)}\frac{\partial h}{\partial y} + F_{j\xi}^{(r)}\frac{\partial\xi}{\partial y} + \tau_x^w D_{j\xi}^{(i)} + \tau_y^w D_{j\xi}^{(r)}\right]\frac{\partial\xi}{\partial y} \\ &+ \left[E_{jh}^{(r)}\frac{\partial h}{\partial x} + E_{jh}^{(i)}\frac{\partial h}{\partial y}\right]\frac{\partial\zeta}{\partial x} - \left[E_{jh}^{(i)}\frac{\partial h}{\partial x} - E_{jh}^{(r)}\frac{\partial h}{\partial y}\right]\frac{\partial\zeta}{\partial y} + \tau_x^w\left[D_{jh}^{(r)}\frac{\partial h}{\partial x} + D_{jh}^{(i)}\frac{\partial h}{\partial y}\right] \\ &+ \tau_y^w\left[D_{jh}^{(r)}\frac{\partial h}{\partial y} - D_{jh}^{(i)}\frac{\partial h}{\partial x}\right] = 0 \qquad j = 1, 2 \end{aligned} \tag{14a}$$

where the superscripts on the coefficients indicate the real or imaginary parts and subscripts ξ and h indicate the derivative of the j^{th} coefficient with respect to $\xi(x, y)$ or $h(x, y)$. The derivatives $E_{j\xi}^{(r)}$, $E_{j\xi}^{(i)}$, and so forth are given in appendix A. Equations (14a) are solved subject to the boundary condition that the volume transport normal to the shore boundary is zero. Thus, if m_1 and m_2 are the x and y components, respectively, of the outward unit normal $\hat{m}$ to the boundary, then for any closed body of water the boundary conditions are

$$M_{jx}m_1 + M_{jy}m_2 = 0 \qquad j = 1, 2 \tag{15a}$$

Equations (14a) and (15a) are the boundary value problem for the solution to a completely enclosed two-layer lake where the thermocline does not intersect the lake bottom or the surface of the lake.

SOLUTION OF THE GOVERNING EQUATIONS

In the previous section the mathematical model for the circulation in a two-layer lake was formulated. The model developed requires the solution of two coupled second-order nonlinear differential equations for the surface displacement ζ and the thermocline position ξ. In a paper to be published, a partial analytical solution in the form of an asymptotic expansion will be given for the case when the vertical eddy diffusivity for momentum ν_{M2} approaches zero. In this report we use finite differences to obtain a solution for equations (14a) subject to the boundary conditions (15a) for parameter values which do not permit use of the asymptotic solution.

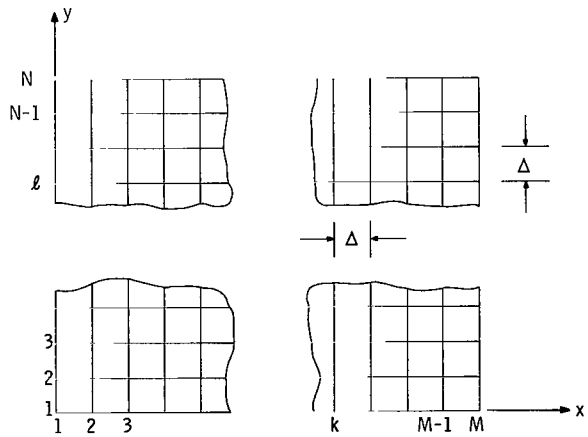

Figure 4. - Numerical grid for rectangular basin.

The point successive underrelaxation iterative method was used to solve the governing equations in a rectangular domain. The equations were linearized about the previous iteration by a Taylor series expansion. The linear finite difference equations at a grid point in the interior for the grid pattern shown in figure 4 are

$$\left[F_j^{(r)}\left(\xi_{k,\ell}^{n}\right)\right]\left(\frac{\xi_{k+1,\ell}^{n}+\xi_{k-1,\ell}^{n+1}-4\xi_{k,\ell}^{n+1}+\xi_{k,\ell-1}^{n+1}+\xi_{k,\ell+1}^{n}}{\Delta^2}\right)$$

$$+\left[E_j^{(r)}\left(\xi_{k,\ell}^{n}\right)\right]\left(\frac{\zeta_{k+1,\ell}^{n}+\zeta_{k-1,\ell}^{n+1}-4\zeta_{k,\ell}^{n+1}+\zeta_{k,\ell-1}^{n+1}+\zeta_{k,\ell+1}^{n}}{\Delta^2}\right)+G_{1j}\left[\frac{\partial\xi}{\partial x}\right]_{f/b}$$

$$+G_{2j}\left[\frac{\partial\xi}{\partial y}\right]_{f/b}+G_{3j}\left[\frac{\partial\zeta}{\partial x}\right]_{f/b}+G_{4j}\left[\frac{\partial\zeta}{\partial y}\right]_{f/b}+G_{5j}\xi_{k,\ell}^{n+1}=G_{6j}\qquad j=1,\ 2 \tag{14b}$$

The G coefficients are listed in appendix B and are all of the form

$$G_{ij}=G_{ij}\left(\xi_{k,\ell}^{n},\ \frac{\xi_{k+1,\ell}^{n}-\xi_{k-1,\ell}^{n+1}}{2\Delta},\ \frac{\xi_{k,\ell+1}^{n}-\xi_{k,\ell-1}^{n+1}}{2\Delta},\ \frac{\zeta_{k+1,\ell}^{n}-\zeta_{k-1,\ell}^{n+1}}{2\Delta},\ \frac{\zeta_{k,\ell+1}^{n}-\zeta_{k,\ell-1}^{n+1}}{2\Delta}\right)$$

Here the previous and present iterations are indicated, respectively, by the superscripts n and n + 1. In these equations central differences with accuracy of order Δ^2 were used for all derivatives except the first derivatives enclosed in the brackets $[\ ]_{f/b}$. For these derivatives either a forward or backward difference with accuracy of order Δ were used depending on which one increases the absolute value of the combined coefficient for $\xi_{k,\ell}^{n+1}$ or $\zeta_{k,\ell}^{n+1}$. Using forward or backward differences to increase the magnitude of the diagonal term in the coefficient matrix was necessary for the iteration scheme to be stable.

For grid points along constant x and y boundaries, the finite difference equations for the equation (15a) boundary condition are

$$E_j^{(r)}\left[\frac{\partial\zeta}{\partial x}\right]_f+F_j^{(r)}\left[\frac{\partial\xi}{\partial x}\right]_f-E_j^{(i)}\left[\frac{\partial\zeta}{\partial y}\right]_{f/b}-F_j^{(i)}\left[\frac{\partial\xi}{\partial y}\right]_{f/b}+G_{7j}\xi_{k,\ell}^{n+1}=G_{8j}\qquad \begin{cases} j=1,\ 2\\ k=1\\ 2\le\ell\le N-1\\ x=0\end{cases} \tag{15b}$$

$$E_j^{(r)}\left[\frac{\partial \zeta}{\partial x}\right]_b + F_j^{(r)}\left[\frac{\partial \xi}{\partial x}\right]_b - E_j^{(i)}\left[\frac{\partial \zeta}{\partial y}\right]_{f/b} - F_j^{(i)}\left[\frac{\partial \xi}{\partial y}\right]_{f/b} + G_{7j}\xi_{k,\ell}^{n+1} = G_{8j} \qquad \begin{cases} j = 1, 2 \\ k = M \\ 2 \le \ell \le N - 1 \\ x = 1 \end{cases} \tag{15c}$$

$$E_j^{(r)}\left[\frac{\partial \zeta}{\partial y}\right]_f + F_j^{(r)}\left[\frac{\partial \xi}{\partial y}\right]_f + E_j^{(i)}\left[\frac{\partial \zeta}{\partial x}\right]_{f/b} + F_j^{(i)}\left[\frac{\partial \xi}{\partial x}\right]_{f/b} + G_{9j}\xi_{k,\ell}^{n+1} = G_{10j} \qquad \begin{cases} j = 1, 2 \\ \ell = 1 \\ 2 \le k \le M - 1 \\ y = 0 \end{cases} \tag{15d}$$

$$E_j^{(r)}\left[\frac{\partial \zeta}{\partial y}\right]_b + F_j^{(r)}\left[\frac{\partial \xi}{\partial y}\right]_b + E_j^{(i)}\left[\frac{\partial \zeta}{\partial x}\right]_{f/b} + F_j^{(i)}\left[\frac{\partial \xi}{\partial x}\right]_{f/b} + G_{9j}\xi_{k,\ell}^{n+1} = G_{10j} \qquad \begin{cases} j = 1, 2 \\ \ell = N \\ 2 \le k \le M - 1 \\ y = 1 \end{cases} \tag{15e}$$

where

$$\left[\frac{\partial \zeta}{\partial x}\right]_f = \frac{\zeta_{k+1,\ell}^{n} - \zeta_{k,\ell}^{n+1}}{\Delta}$$

$$\left[\frac{\partial \zeta}{\partial y}\right]_b = \frac{\zeta_{k,\ell}^{n+1} - \zeta_{k-1,\ell}^{n}}{\Delta}$$

. .
. .
. .

The G_{8j} to G_{10j} coefficients are given in appendix B and are functions of the n^{th} iteration value of ξ and ζ. For the derivatives tangential to the boundary in equations (15b) to (15e), either forward or backward difference was used depending on which one made the total coefficient of $\xi_{k,\ell}$ and $\zeta_{k,\ell}$ maximum. Equations (15b), (15c), (15d), and (15e) were used respectively for the corner points 1, 1; M, N; N, 1; and 1, M with the proper difference equation substituted for the first derivatives tangential to the boundaries.

Equations (14b) and (15b) to (15e) constitute a set of equations for $\xi^{n+1}_{k,\ell}$ and $\zeta^{n+1}_{k,\ell}$ at a mesh point. Every iteration, the equations were solved simultaneously for $\xi^{n+1}_{k,\ell}$ and $\zeta^{n+1}_{k,\ell}$ at every grid point. The standard relaxation procedure was then applied with the relaxation coefficient usually taken to be 0.5. In performing the calculations it was necessary to have at one point on the boundary a specific ζ and ξ value. In order to accomplish this the difference between the new value at the boundary point and the desired value was either subtracted or added to the entire ζ and ξ field after each iteration. The iteration process was continued until the maximum ζ and ξ relative error between successive iterations at any point was less than 1.0×10^{-4}.

It should be realized that the equations we are solving are highly nonlinear. The numerical procedure used to solve the equations (particularly the use of underrelaxation and the use of forward or backward differences to make the solution matrix diagonally dominate) was not known a priori but was developed empirically. Because the coefficients in the equations that must be calculated every iteration are so complicated, each iteration takes a considerable length of time to perform. For a grid mesh of $\Delta = 0.1$ (121 grid points over the lake region) a typical solution takes 20 to 40 minutes to obtain on an IBM 7090 system if the poor initial ξ and ζ distributions of a constant are used to start the calculation.

RESULTS

The finite difference equations (14b) and (15b) to (15e) were solved for the position of the thermocline ξ and the position of the lake surface ζ. Using the solutions for ξ and ζ, equations (8) and (9) determine the hypolimnion and epilimnion horizontal velocities.

Effect of Eddy Diffusivities

In this section the effect of variation of the hypolimnion and epilimnion eddy diffusivities will be discussed. The results to be presented will all be for a constant depth square basin with the following parameter values being held constant:

Basin length, L, km	96.6
Basin depth, H, m	62.6
Epilimnion temperature, ^{o}C	22
Hypolimnion temperature, ^{o}C	4
$\Delta\rho$	0.00203
ρ_r	0.9977969
Wind velocity at 6 meters above water surface, m/sec	5.2
τ_x^w, dynes/cm^2	-0.914
τ_y^w, dynes/cm^2	0.0

A drag coefficient of 0.00273 as proposed by Wilson (ref. 10) was used to determine the wind shear stress for the 5.2-meter-per-second wind. The values listed previously are typical for the central basin of Lake Erie.

Case 1

In the first case to be discussed the eddy diffusivities used in the epilimnion and hypolimnion are respectively $\nu_{M1} = 16.8$ square centimeters per second and $\nu_{M2} = 4.2$ square centimeters per second. These eddy diffusivities correspond to friction depths of $d_1 = 18.2$ meters and $d_2 = 9.1$ meters. The wind drag coefficient and ν_{M1} value used here are the same as the ones used by Gedney (refs. 8 and 9) for current calculations in Lake Erie with uniform water temperature (no stratification). With these values for ν_{M1} and the drag coefficient, the calculated velocities for Lake Erie agreed very well with measurements. The epilimnion in our model is considered to be of uniform temperature and for the cases calculated here will have an average thickness of approximately 20 meters. Since 20 meters is also near the average depth of Lake Erie, the ν_{M1} value should be very similar to that used in the Lake Erie calculations. The value of ν_{M2} in this first case is somewhat arbitrary. Results for different values of ν_{M2} will be reported in subsequent cases.

Constant thermocline (ξ) contours when $\nu_{M1} = 16.8$ and $\nu_{M2} = 4.2$ are shown in figure 5(a). The thermocline assumes a shallow depth at the upwind end of the lake and a large depth at the downwind end. There is very little tilting of the thermocline in the cross wind direction. At a constant x station, the thermocline is deeper in the center of the lake than near the shores. The value of $\partial\xi/\partial n + \partial\zeta/\partial n$ throughout the basin is very close to zero. The thermocline therefore assumes a position so that the horizontal pressure gradient $\partial P_2/\partial N$ in the hypolimnion is close to zero. With $\partial P_2/\partial N$ being small, the velocities in the hypolimnion should also be small.

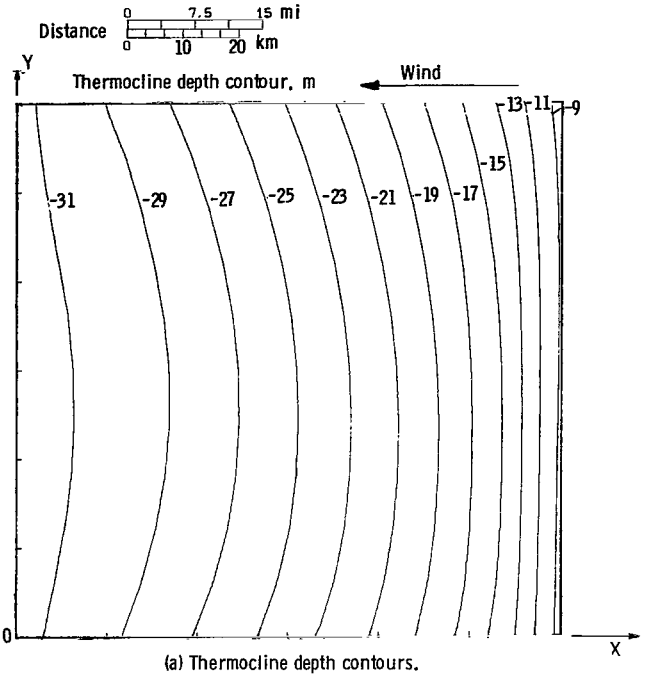

(a) Thermocline depth contours.

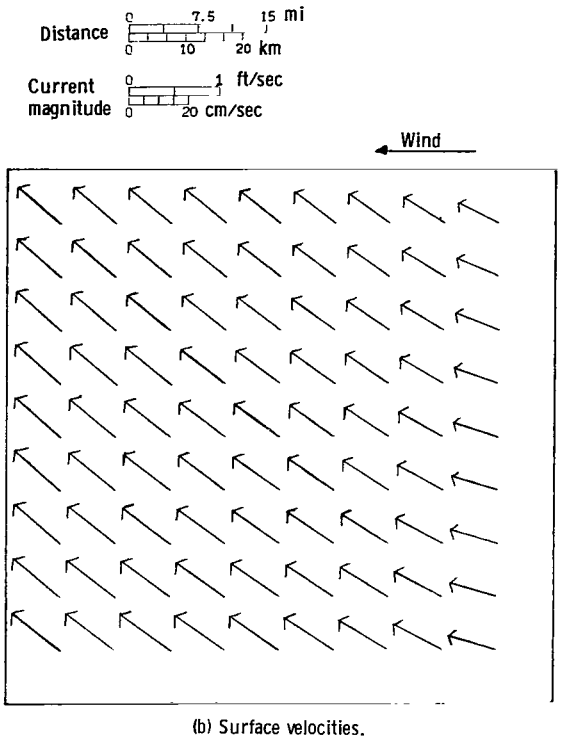

(b) Surface velocities.

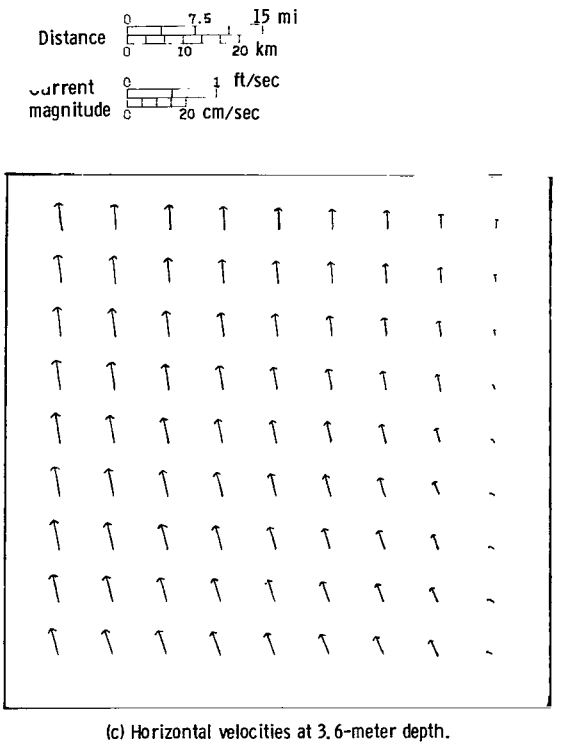

(c) Horizontal velocities at 3.6-meter depth.

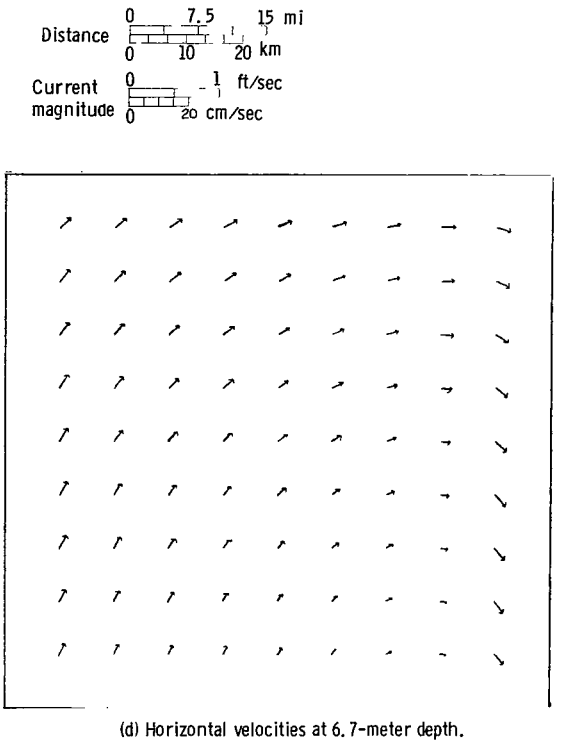

(d) Horizontal velocities at 6.7-meter depth.

Figure 5. - Circulation in a two-layer basin of constant depth. Lake length, 96.6 kilometers; ν_{M1} = 16.8 square centimeters per second; ν_{M2} = 4.2 square centimeters per second.

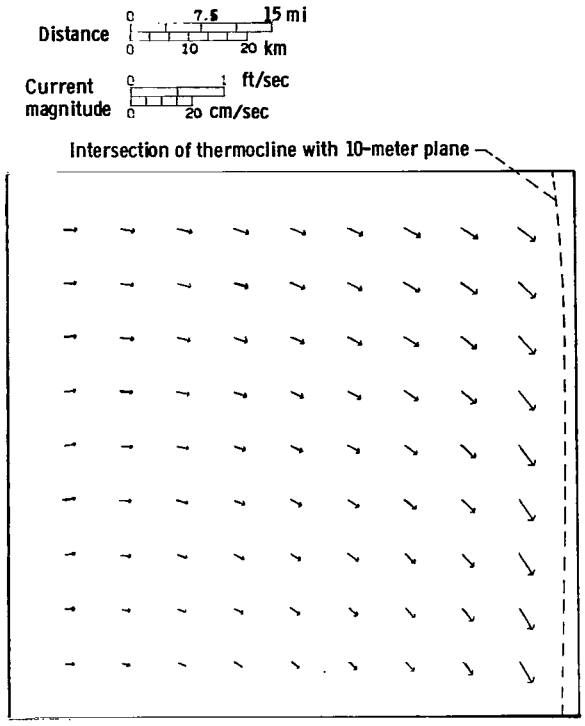

(e) Horizontal velocities at 10-meter depth.

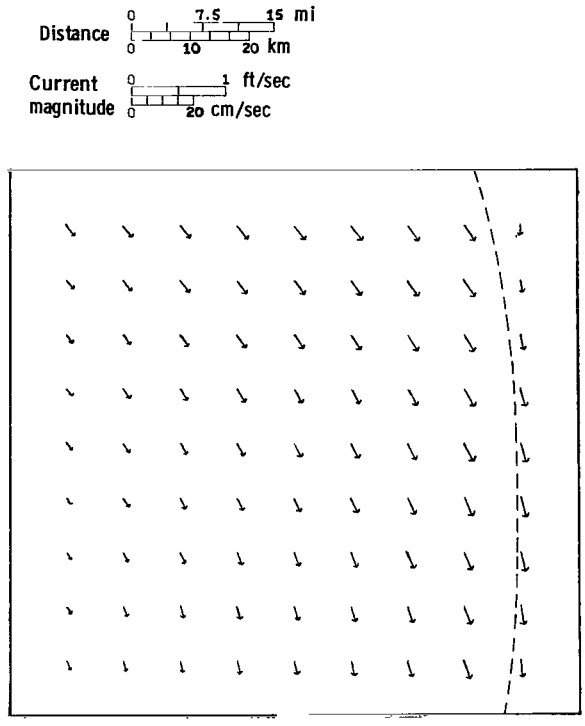

(f) Horizontal velocities at 15-meter depth.

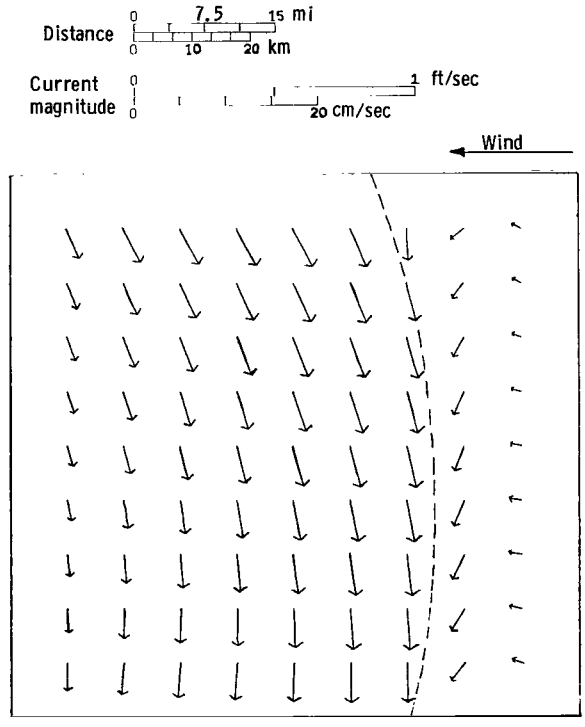

(g) Horizontal velocities at 20-meter depth.

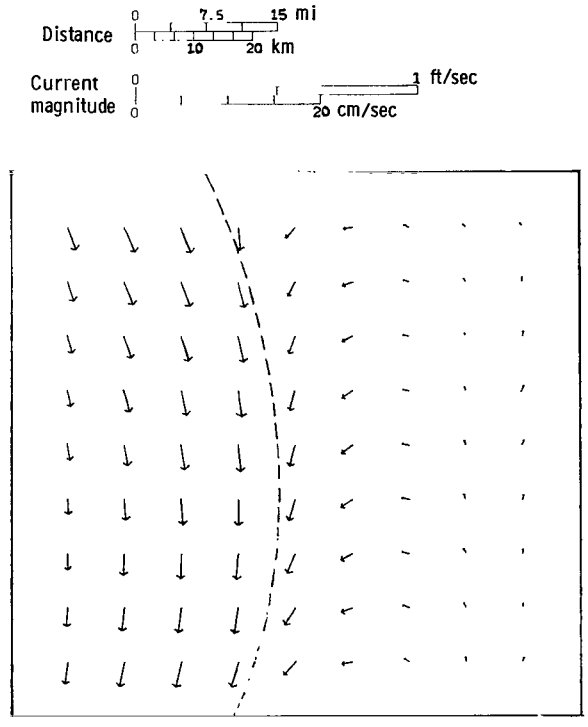

(h) Horizontal velocities at 26-meter depth.

Figure 5. - Continued.

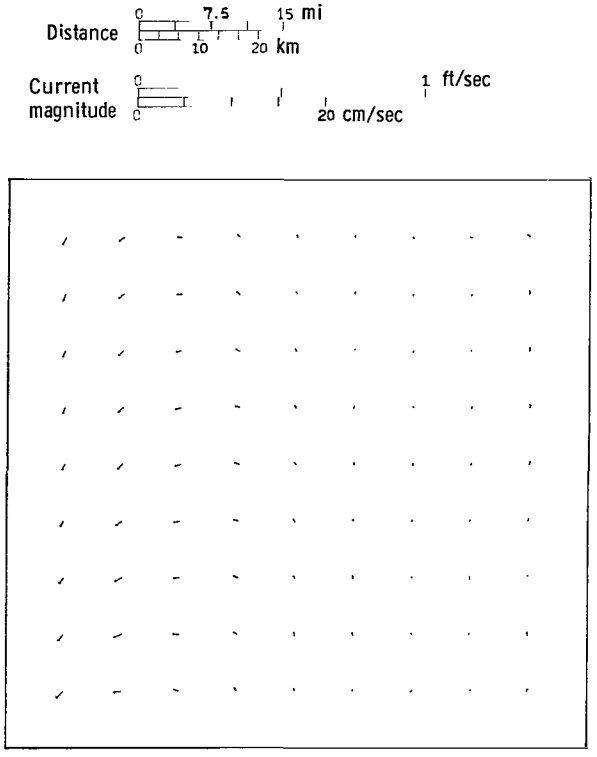

(i) Horizontal velocities at 32-meter depth.

Figure 5. - Concluded.

In figures 5(b) to (i), the horizontal velocities are given at the lake surface and at depths of 3.6, 6.7, 10.0, 15.0, 20.0, 26.0, and 32.0 meters. The dashed line included on some of the velocity plots is the intersection of the thermocline with the horizontal plane at that particular depth. The velocity patterns down to 10 meters are similar to those which occur in a homogeneous lake. The Coriolis force causes the deflection of the surface velocities to the right of the wind and a clockwise rotation of the current vector with depth. The effect of the epilimnion thickness being smaller at the upwind end of the lake causes the upwind velocities at the surface (fig. 5(b)) to be more in the direction of the wind. At depths closer to the thermocline, the epilimnion velocities rotate even more clockwise until they are in a southerly crosswind direction. As we go deeper to a region below the thermocline, the velocities become very small and aline themselves to the right of the wind. The velocity magnitudes at 32 meters are only 2 to 3 percent of those at the surface. Note that the apparent increase in velocity between figures 5(f) and (g) only reflects a scale change.

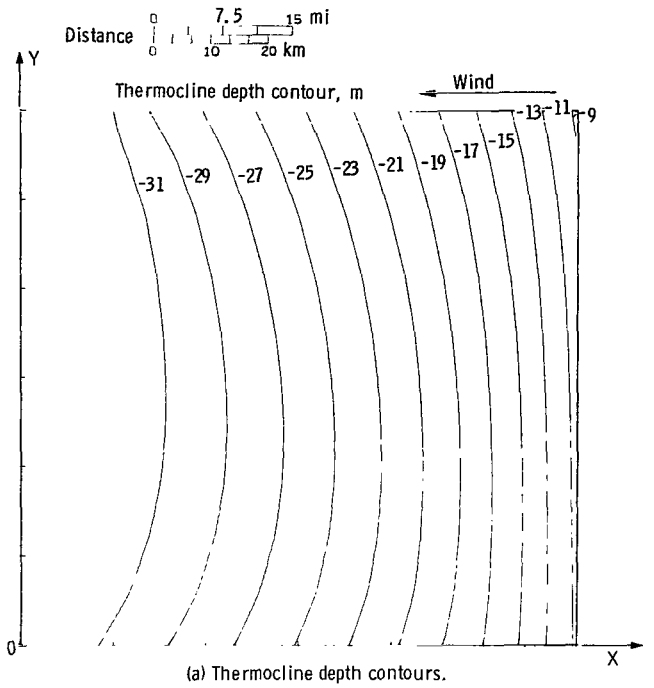

(a) Thermocline depth contours.

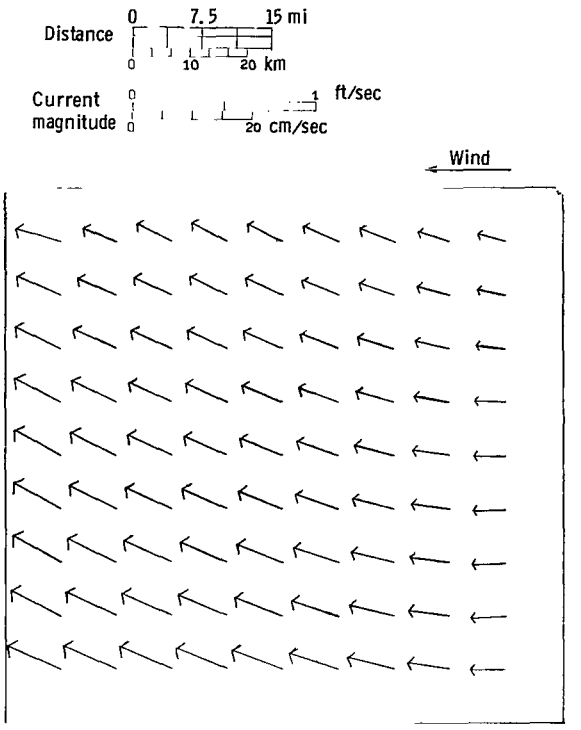

(b) Surface velocities.

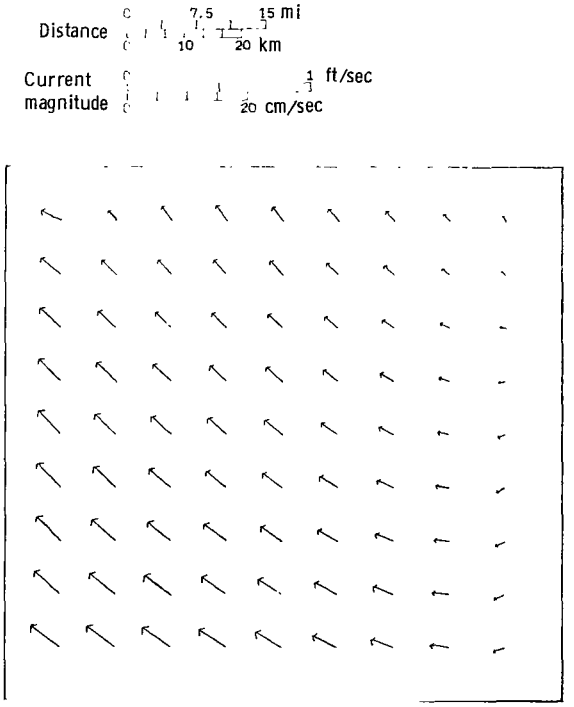

(c) Horizontal velocities at 3.6-meter depth.

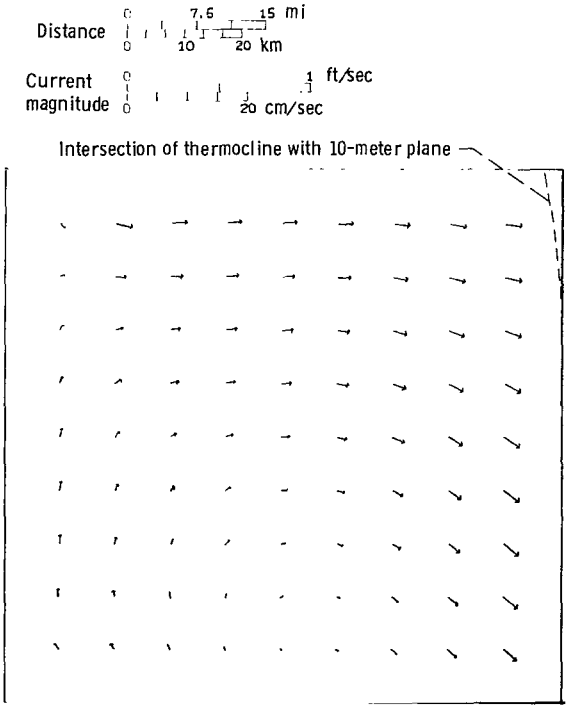

(d) Horizontal velocities at 10-meter depth.

Figure 6. - Circulation in a two-layer basin of constant depth. Lake length, 96.6 kilometers; ν_{M1} = 67.2 square centimeters per second; ν_{M2} = 16.8 square centimeters per second.

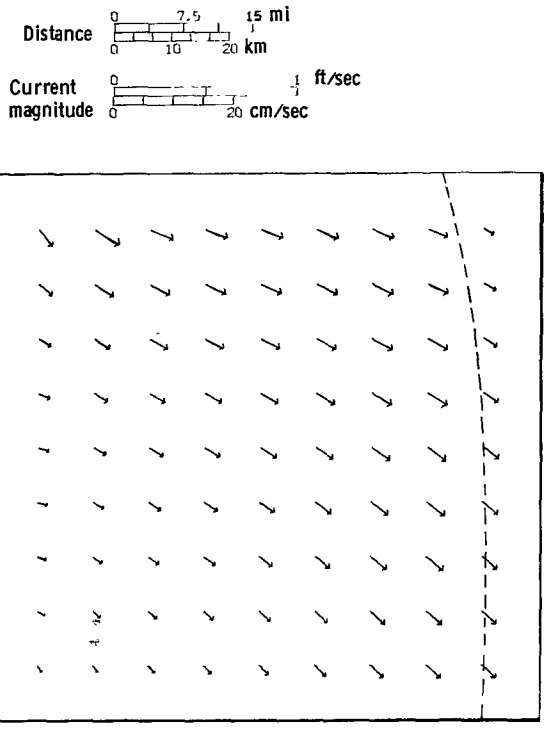

(e) Horizontal velocities at 15-meter depth.

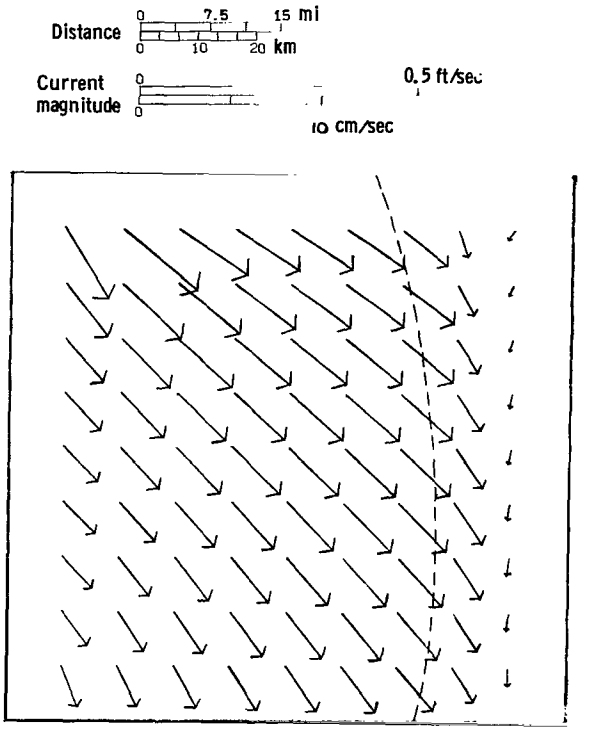

(f) Horizontal velocities at 20-meter depth.

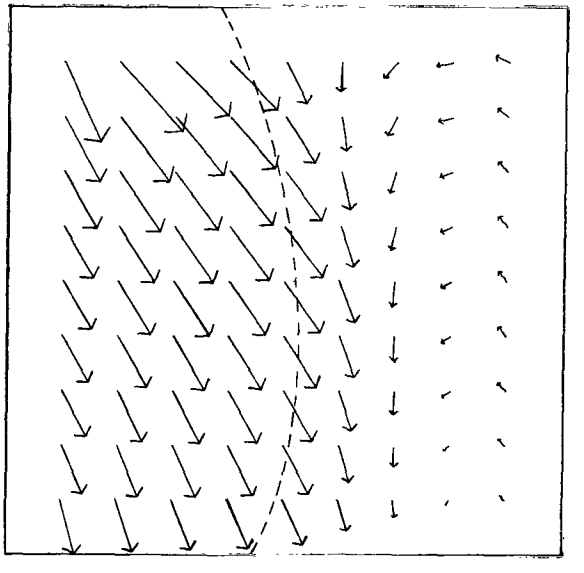

(g) Horizontal velocities at 26-meter depth.

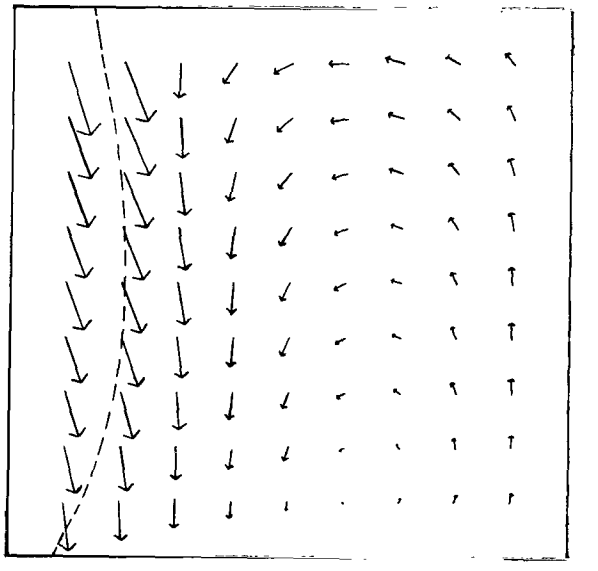

(h) Horizontal velocities at 32-meter depth.

Figure 6. - Concluded.

Case 2

Results are given in figure 6 for the same parameters in case 1 except ν_{M1} and ν_{M2} are quadrupled to be, respectively, 67.2 and 16.8 square centimeters per second. For comparison purposes the same thermocline depth at the upper righthand corner have been used in both cases 1 and 2. As shown in figure 6(a) the larger eddy viscosities produce a greater crosswind thermocline tilt and maximum thermocline depth. As shown by figures 6(b) to (d) the velocities in the upper part of the epilimnion are approximately one-half that of the case 1 results. This is the same order of magnitude velocity change that occurs when the eddy diffusivity for a shallow ($H/d_1 \leq 1$) homogeneous lake is quadrupled. The significant result is that the velocities below the thermocline are larger than those in case 1 reflecting the increase in momentum transport across the thermocline because of the large eddy diffusivities.

Case 3

The effect of changing ν_{M2} as ν_{M1} is held constant is shown in figure 7 which is a plot of the thermocline depth along the $y = 0$ axis. With $\nu_{M1} = 16.8$ square centimeters per second, plots are shown for $\nu_{M2} = 4.2$ and 1.05 square centimeters per second. We see, as $\nu_{M2} \to 0$, the difference between the thermocline depth at $x = 0$ and $x = 1$ becomes less. In addition, as $\nu_2 \to 0$: (1) the cross wind tilt of the thermo-

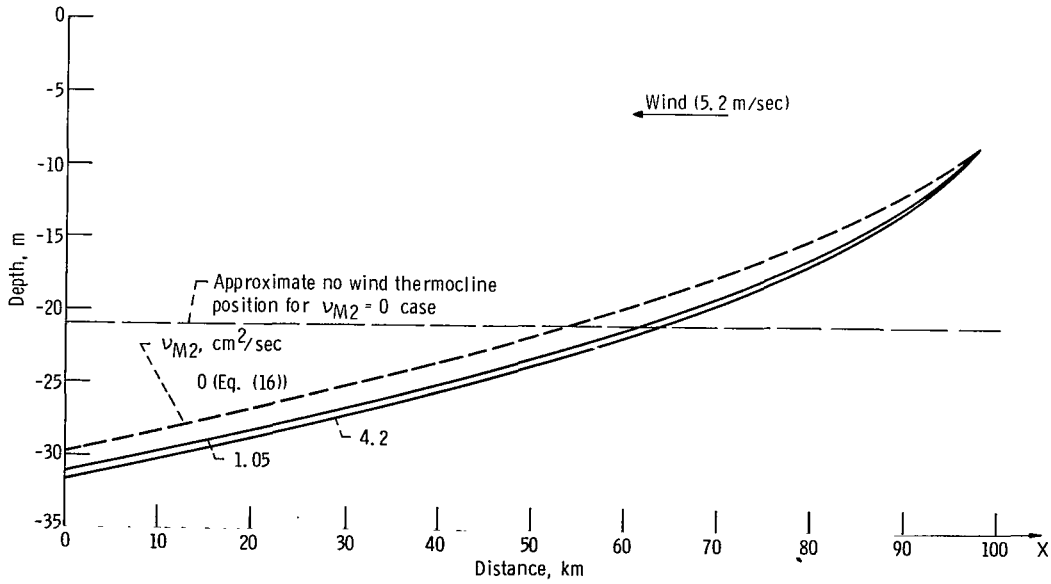

Figure 7. - Thermocline position at $y = 0$ for $\nu_{M2} = 0.0$, 1.05, and 4.2 square centimeters per second and $\nu_{M1} = 16.8$ square centimeters per second.

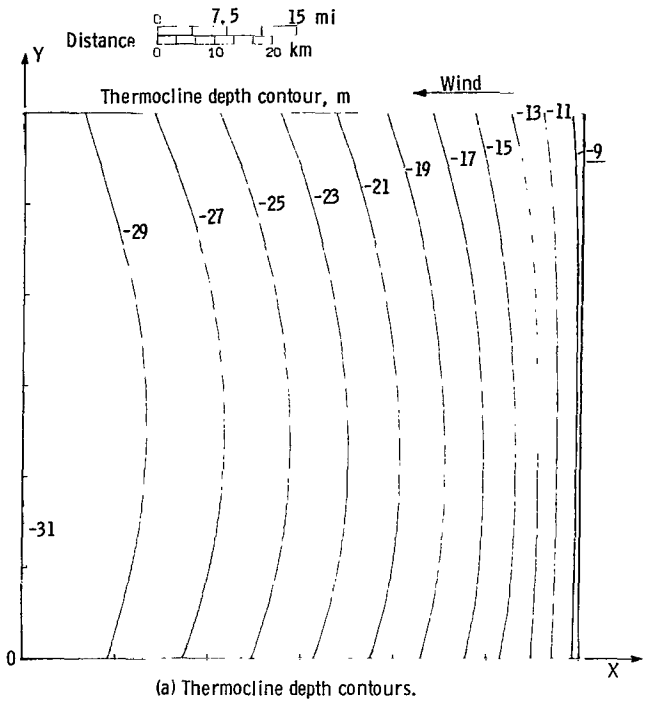

(a) Thermocline depth contours.

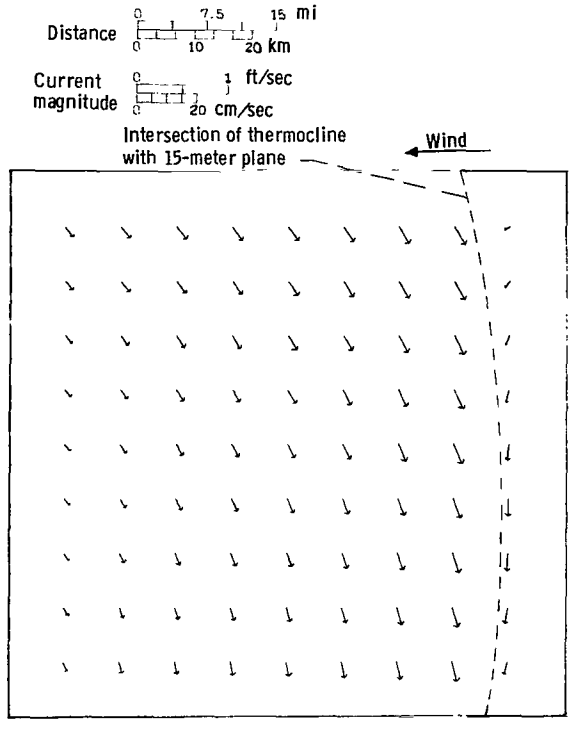

(b) Horizontal velocities at 15-meter depth.

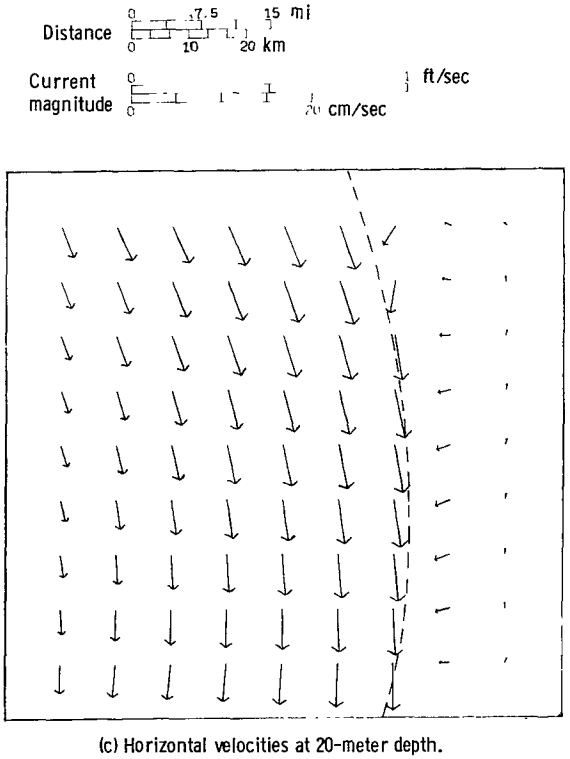

(c) Horizontal velocities at 20-meter depth.

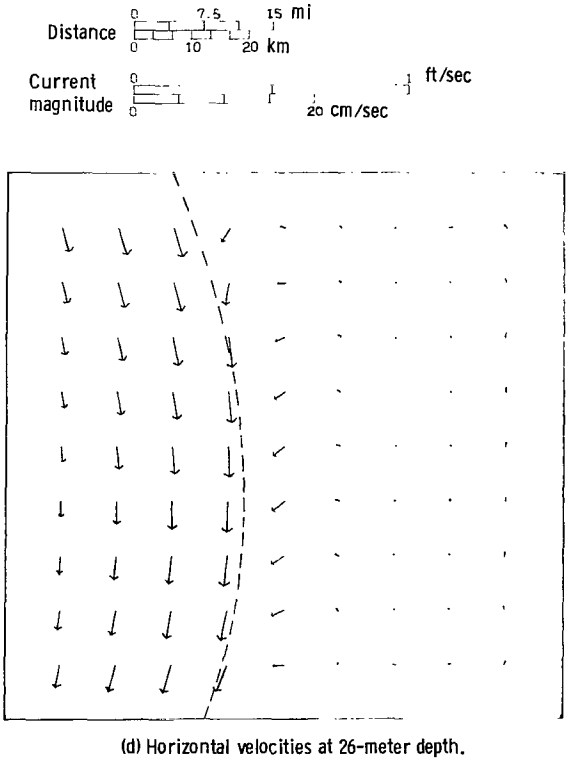

(d) Horizontal velocities at 26-meter depth.

Figure 8. - Circulation in a two-layer basin of constant depth. Lake length, 96.6 kilometers; ν_{M1} = 14.8 square centimeters per second; ν_{M2} = 1.05 square centimeters per second.

cline becomes smaller; (2) the thermocline depth distribution along $x = 0$ and $x = 1$ becomes independent of y; and (3) the thermocline distribution as a function of x along $y = 0$ and $y = 1$ become the same. These characteristics are shown in the figure 8(a) thermocline contour plot for the case when $\nu_{M2} = 1.05$ square centimeters per second.

The velocities at 15, 20, and 26 meters are shown, respectively, on figures 8(b) to (d) when $\nu_{M1} = 14.8$ square centimeters per second and $\nu_{M2} = 1.05$ square centimeters per second. The velocities below the thermocline can be seen to be smaller than those in case 1 where $\nu_{M1} = 14.8$ and $\nu_{M2} = 4.2$.

Comparison With Asymptotic Limit

As $\nu_{M2} \to 0$ it is possible to construct an asymptotic expansion of the governing equations (10) and (11) in terms of the small parameter

$$\kappa_\tau = \frac{d_2}{d_1}\frac{1}{\rho_r}$$

A zeroth-order solution for the thermocline was obtained and will be completely given in a future report. The zeroth-order thermocline position along the boundaries of a rectangular basin with $\tau_y^w = 0$ and constant $\tau_x^w < 0$ is

$$\bar{\xi} = \begin{cases} \bar{\xi}_1 = \text{constant} & \text{at } X = L \\ -\sqrt{\dfrac{-2L\bar{\tau}_x^w}{(\rho_2 - \rho_1)g} + |\bar{\xi}_1|^2} & \text{at } X = 0 \\ -\sqrt{\dfrac{2(X - L)\bar{\tau}_x^w}{(\rho_2 - \rho_1)g} + |\bar{\xi}_1|^2} & \text{at } Y = 0,\ \beta L \end{cases} \qquad (16)$$

where β is the width to length ratio of the basin. This solution predicts the zeroth-order thermocline position on the boundaries independent of β, ν_{M1}, ν_{M2}, and h. It should be noted that the asymptotic solution is only valid when $e^{-\alpha_2/2(h+\xi)} \ll \kappa_\tau$. For $\nu_{M2} \leq 1.05$ square centimeters per second, this approximation is valid provided the

thermocline never approaches within a few meters of the lake bottom. The asymptotic solution interior to the boundaries does, however, depend on β, ν_{M1}, ν_{M2}, and the lake depth h.

Included in figure 7 is a plot of equation (16). The numerical solutions approach the asymptotic results as ν_{M2} decreases. It should also be noted that the zeroth-order expansion gives the result that

$$\frac{\partial \xi}{\partial n} + \frac{\partial \zeta}{\partial n} = 0$$

in the entire lake domain. The numerical solution gives $\partial\xi/\partial n + \partial\zeta/\partial n$ of order 10^{-2} for $\nu_{M2} = 1.05$ square centimeters per second. This agreement between the zeroth-order asymptotic and numerical solution is good since the first-order term in the asymptotic expansion would be of this magnitude.

In figure 9 the thermocline positions for the zeroth-order asymptotic solution and the $\nu_2 = 4.2$ square centimeters per second numerical solution are given when the epilimnion water volume are approximately equal in both cases.

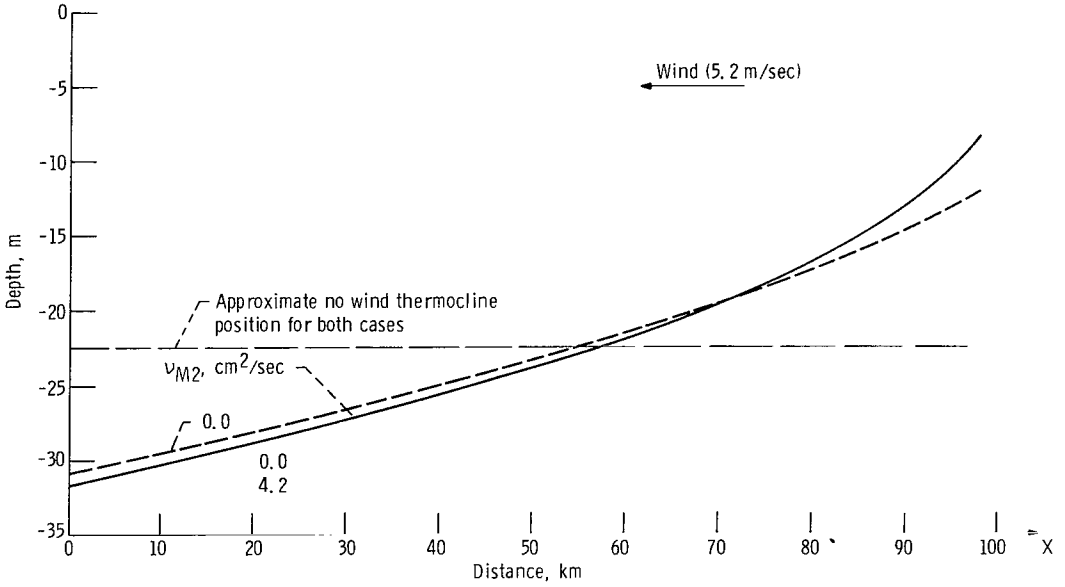

Figure 9. - Thermocline position at y = 0 for ν_{M2} = 0.0 and 4.2 square centimeters per second and ν_{M1} = 16.8 square centimeters per second with equal epilimnion volume.

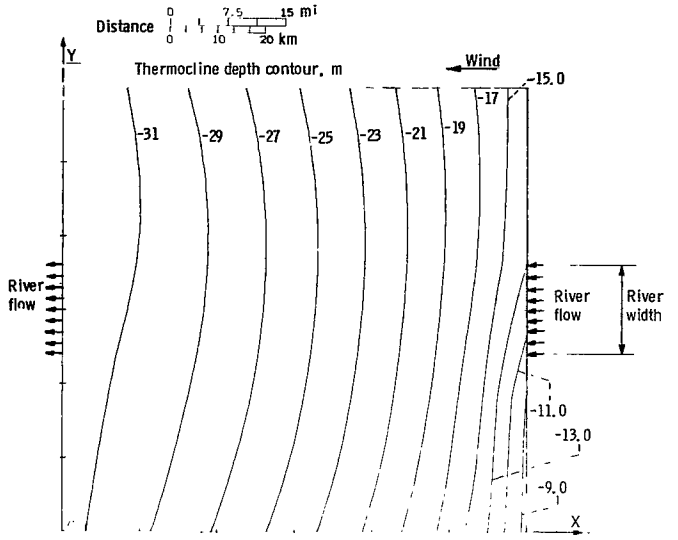

(a) Thermocline depth contours.

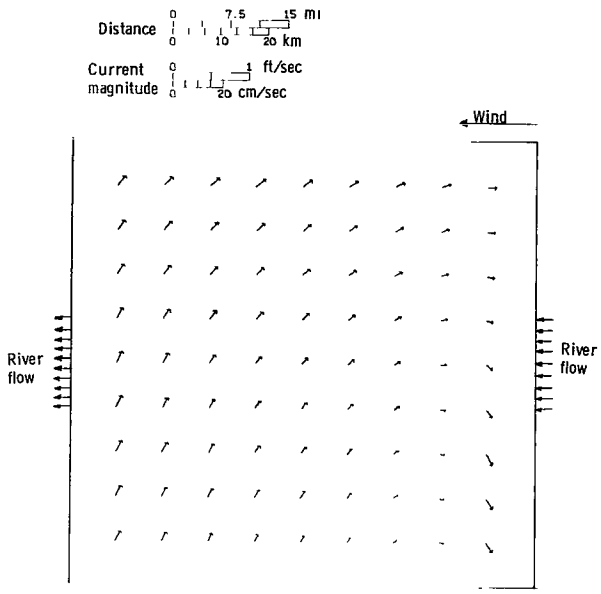

(b) Horizontal velocities at 6.7-meter depth.

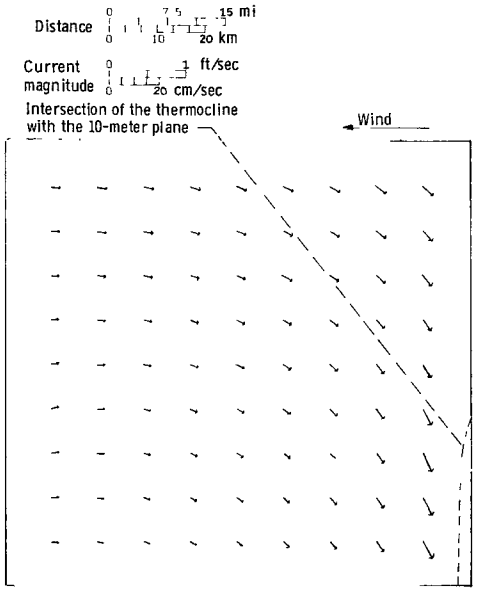

(c) Horizontal velocities at 10-meter depth.

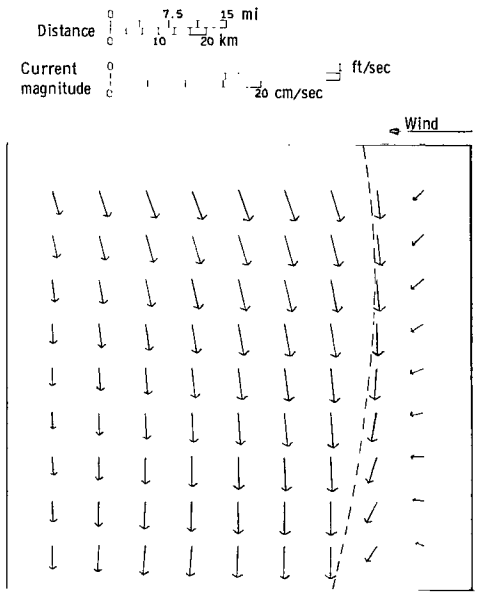

(d) Horizontal velocities at 20-meter depth.

Figure 10. - Circulation in a two-layer basin of constant depth with river flow. Lake length, 96.6 kilometers; ν_{M1} = 14.8 square centimeters per second; ν_{M2} = 4.2 square centimeters per second.

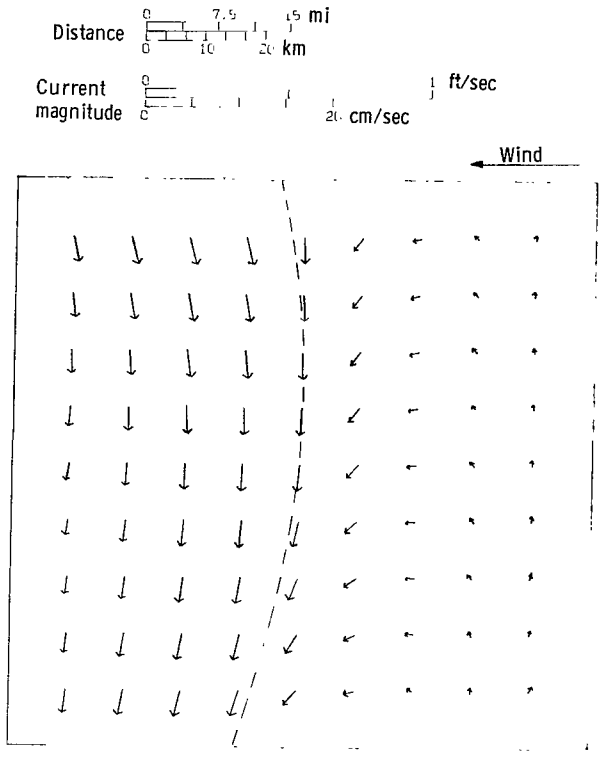

(e) Horizontal velocities at 25-meter depth.

Figure 10. - Concluded.

Effect of Varying Other Parameters

The effects of varying the hypolimnion and epilimnion eddy diffusivities has been given in the previous sections. The effect of changes in τ^W, L, $\Delta\rho$, and epilimnion water volume can produce large changes in thermocline slope. The qualitative effects of these parameters are easily deduced from the asymptotic solution given in equation (16) and were confirmed by the numerical solution for the case when $\nu_2 = 16.8$ square centimeters per second and $\nu_1 = 4.2$ square centimeters per second.

Changing the lake depth produced no significant change in the thermocline position until the distance between the lake bottom and the thermocline is less than the hypolimnion friction depth d_2. When $H + \overline{\xi}$ is made less than d_2 for a constant depth basin, the thermocline slope increases until the thermocline intersected the lake bottom. Including a bottom slope where $H + \overline{\xi}$ was made small did not change this behavior.

A plot of the thermocline position for the same parameters as case 1 shown in figure 5 but including an east to west river flow of 5380 cubic meters per second is shown in figure 10. This river through-flow which is similar in magnitude to that in Lake Erie occurs in the epilimnion only. The main effect of the through-flow is to increase the

crosswind tilt of the thermocline. A through-flow of equal but opposite direction would produce an opposite crosswind tilt of the thermocline. Some velocities for the east to west through-flow are included in figure 10. The river flow effect on the velocities is quite small being most significant at the upwind end of the lake where the epilimnion thickness is the smallest.

CONCLUSIONS

The solution of the two-layer lake equations in a rectangular basin with a uniform 5.2-meter-per-second steady wind was solved for the case when the thermocline does not intercept the bottom or surface of the lake. The velocity and shear stress was made continuous across the thermocline. The density difference between the two layers was assumed to be 0.00203 gram per cubic centimeter. The following conclusions were determined from the results of the numerical solution:

1. The major tilt of the thermocline occurs in the direction of the wind with the maximum thermocline depth being at the downwind end of the lake.

2. In the Northern Hemisphere, a small crosswind tilt of the thermocline occurs with the depth of the thermocline to the right of the wind being less than that to the left.

3. As the eddy diffusivity in the hypolimnion is decreased the thermocline tilt and hypolimnion velocities decrease. For the range of hypolimnion diffusivities investigated (1.05 to 16.8 cm^2/sec), the pressure gradient in the hypolimnion was always found to be small (of order 10^{-2}).

4. The shape of the thermocline was found to be weakly dependent on the length to width ratio and depth of the lake. As a result, most of the results are given for a square basin.

5. As the hypolimnion eddy diffusivity is reduced, the numerical solution approaches an asymptotic solution which assumes the ratio of hypolimnion to epilimnion diffusivities to be much less than one. The zeroth-order asymptotic solution predicts the thermocline slope to be directly proportional to the wind shear stress and basin length and inversely proportional to the density difference of the two layers and the local thermocline depth.

6. Since the crosswind variation in the thermocline depth is small, the thermocline can be approximated by a cylindrical surface generated from a single curve.

Lewis Research Center,
National Aeronautics and Space Administration,
Cleveland, Ohio, March 22, 1972,
136-13.

APPENDIX A

COEFFICIENTS FOR THE DIFFERENTIAL EQUATIONS

$$D_1 = \frac{1}{\omega^2}\left[1 - \frac{2\kappa_\tau\left(1 + e^{-2a_2}\right)e^{a_1}}{K}\right]$$

$$E_1 = 2i\left[-\alpha_1\xi + \frac{2\rho_r\kappa_\tau\left(e^{2a_1} - 1\right)e^{-a_2}}{K\omega} + \rho_r\frac{\kappa_\tau\,\Delta\rho}{K\omega}\left(e^{2a_1} - 1\right)\left(1 + e^{-2a_2}\right)\right]$$

$$F_1 = E_1 + 2i\alpha_1\xi - \frac{2i\kappa_\tau}{K\omega}\left(1 + e^{-2a_2}\right)\left(e^{2a_1} - 1\right)$$

$$D_2 = -\frac{4}{K\omega^2}\left[e^{-a_2} - \frac{1}{2}\left(1 + e^{-2a_2}\right)\right]e^{a_1}$$

$$E_2 = \frac{2i}{K\omega}\left\{2\rho_r\,\Delta\rho\left[e^{-a_2} - \frac{1}{2}\left(1 + e^{-2a_2}\right)\right]\left(e^{2a_1} - 1\right)\right.$$

$$\left. + \rho_r\left[(a_2 + 1)K + 2\left(1 - e^{-a_2}\right)\left(e^{2a_1} - 1\right) - 2\kappa_\tau\left(e^{2a_1} + 1\right)\right]\right\}$$

$$F_2 = E_2 - \frac{4i}{K\omega}\left[e^{-a_2} - \frac{1}{2}\left(1 + e^{-2a_2}\right)\right]\left(e^{2a_1} - 1\right)$$

$$D_{1\xi} = \frac{\partial D_1}{\partial\xi} = -\left(D_1\omega - \frac{1}{\omega}\right)\frac{C_K}{K} - \frac{2\kappa_\tau e^{a_1}}{K\omega}\left[\alpha_1 + e^{-2a_2}(\alpha_1 - 2\alpha_2\right]$$

$$C_K = \frac{1}{\omega}\frac{\partial K}{\partial\xi} = -2\left\{\kappa_\tau\left[\alpha_2 e^{-2a_2}\left(1 + e^{2a_1}\right) - \alpha_1 e^{2a_1}\left(1 + e^{-2a_2}\right)\right]\right.$$

$$\left. + \alpha_1 e^{2a_1}\left(1 - e^{-2a_2}\right) + \alpha_2 e^{-2a_2}\left(e^{2a_1} - 1\right)\right\}$$

$$E_{1\xi} = \frac{\partial E_1}{\partial \xi} = -2i\alpha_1 + 2i\kappa_\tau \left\{ \Delta\rho\ \rho_r DSCK + \frac{2\rho_r e^{-a_2}}{K} \left[-\left(\frac{C_K}{K} + \alpha_2\right)\left(e^{2a_1} - 1\right) + 2\alpha_1 e^{2a_1} \right] \right\}$$

$$DSCK = \frac{1}{\omega}\frac{\partial}{\partial \xi}\left[\frac{\left(e^{2a_1} - 1\right)\left(1 + e^{-2a_2}\right)}{K}\right]$$

$$DSCK = \frac{1}{K}\left[2\alpha_1 e^{2a_1}\left(1 + e^{-2a_2}\right) - 2\alpha_2 e^{-2a_2}\left(e^{2a_1} - 1\right) - \frac{C_K}{K}\left(e^{2a_1} - 1\right)\left(1 + e^{-2a_2}\right)\right]$$

$$F_{1\xi} = E_{1\xi} + 2i\alpha_1 - 2i\kappa_\tau DSCK$$

$$D_{2\xi} = -\frac{\omega D_2 C_K}{K} - \frac{4e^{a_1}}{K\omega}\left[e^{-a_2}(\alpha_1 - \alpha_2) + e^{-2a_2}\left(\alpha_2 - \frac{1}{2}\alpha_1\right) - \frac{1}{2}\alpha_1\right]$$

$$E_{2\xi} = -\frac{E_2 \omega C_K}{K} + \frac{2i}{K}\left(2\rho_r \Delta\rho \left\{2\alpha_1 e^{2a_1}\left[e^{-a_2} - \frac{1}{2}\left(1 + e^{-2a_2}\right)\right]\right.\right.$$

$$\left. + \alpha_2\left(-e^{-a_2} + e^{-2a_2}\right)\left(e^{2a_1} - 1\right)\right\} + \rho_r \left\{\alpha_2 K + (a_2 + 1)C_K\right.$$

$$\left.\left. + 2e^{-a_2}\left[\alpha_2\left(e^{2a_1} - 1\right) - 2\alpha_1 e^{2a_1}\right] - 4.0\ \alpha_1 e^{2a_1}(\kappa_\tau - 1)\right\}\right)$$

$$F_{2\xi} = E_{2\xi} - \omega(F_2 - E_2)\frac{C_K}{K} - \frac{4i}{K}\left\{\alpha_2\left(e^{2a_1} - 1\right)\left(-e^{-a_2} + e^{-2a_2}\right)\right.$$

$$\left. + 2\alpha_1 e^{2a_1}\left[e^{-a_2} - \frac{1}{2}\left(1 + e^{-2a_2}\right)\right]\right\}$$

$$D_{1h} = \frac{\alpha_2}{K\omega}\left[4\kappa_\tau e^{a_1} e^{-2a_2} - K_h\left(\frac{iD_1}{2} - 1\right)\right]$$

$$K_h = -2e^{-2a_2}\left[\kappa_\tau\left(1 + e^{2a_1}\right) + \left(e^{2a_1} - 1\right)\right] = \frac{1}{\alpha_2\omega}\frac{\partial K}{\partial h}$$

$$E_{1h} = -\frac{K_h\omega\alpha_2}{K}(E_1 + 2i\alpha_1\xi) + \frac{4i\kappa_\tau\alpha_2}{K}\left[\left(e^{2a_1} - 1\right)\left(-\rho_r\,\Delta\rho\, e^{-2a_2} - \rho_r e^{-a_2}\right)\right]$$

$$F_{1h} = E_{1h} + \frac{2i\alpha_2\kappa_\tau\left(e^{2a_1} - 1\right)}{K}\left[2e^{-2a_2} + \frac{K_h}{h}\left(1 + e^{-2a_2}\right)\right]$$

$$D_{2h} = -\frac{\alpha_2}{K}\left[D_2K_h\omega + \frac{4}{\omega}\left(-e^{-a_2} + e^{-2a_2}\right)e^{a_1}\right]$$

$$E_{2h} = \frac{\alpha_2}{K}\left\{-K_h\omega E_2 + 2i\rho_r\left[2e^{-a_2}\left(e^{2a_1} - 1\right) + K_h(a_2 + 1) + K\right]\right.$$

$$\left. + 4i\rho_r\,\Delta\rho\left(-e^{-a_2} + e^{-2a_2}\right)\left(e^{2a_1} - 1\right)\right\}$$

$$F_{2h} = E_{2h} - \alpha_2(F_2 - E_2)\frac{K_h}{K}\omega - \frac{4i\alpha_2}{K}\left(e^{-2a_2} - e^{-a_2}\right)\left(e^{2a_1} - 1\right)$$

APPENDIX B

COEFFICIENTS FOR THE DIFFERENCE EQUATIONS

In this appendix the coefficients D_j, E_j, F_j, and their derivatives are all evaluated at $\xi^n_{k,\ell}$ and the local h value.

$$G_{1j} = E^{(r)}_{j\xi}\frac{\partial \zeta^n}{\partial x} - E^{(i)}_{j\xi}\frac{\partial \zeta^n}{\partial y} + 2F^{(r)}_{j\xi}\frac{\partial \xi^n}{\partial x} + \tau^w_x D^{(r)}_{j\xi} - \tau^w_y D^{(i)}_{j\xi} + F^{(r)}_{jh}\frac{\partial h}{\partial x} + F^{(i)}_{jh}\frac{\partial h}{\partial y}$$

$$G_{2j} = E^{(i)}_{j\xi}\frac{\partial \zeta^n}{\partial x} + E^{(r)}_{j\xi}\frac{\partial \zeta^n}{\partial y} + 2F^{(r)}_{j\xi}\frac{\partial \xi^n}{\partial y} + \tau^w_x D^{(i)}_{j\xi} + \tau^w_y D^{(r)}_{j\xi} + F^{(r)}_{jh}\frac{\partial h}{\partial y} - F^{(i)}_{jh}\frac{\partial h}{\partial x}$$

$$G_{3j} = E^{(r)}_{j\xi}\frac{\partial \xi^n}{\partial x} + E^{(i)}_{j\xi}\frac{\partial \xi^n}{\partial y} + E^{(r)}_{jh}\frac{\partial h}{\partial x} + E^{(i)}_{jh}\frac{\partial h}{\partial y}$$

$$G_{4j} = E^{(r)}_{j\xi}\frac{\partial \xi^n}{\partial y} - E^{(i)}_{j\xi}\frac{\partial \xi^n}{\partial x} + E^{(r)}_{jh}\frac{\partial h}{\partial y} - E^{(i)}_{jh}\frac{\partial h}{\partial x}$$

$$\begin{aligned} G_{5j} = {} & F^{(r)}_{j\xi}\nabla^2\xi^n + E^{(r)}_{j\xi}\nabla^2\zeta^n + \left[E^{(r)}_{j\xi\xi}\frac{\partial \zeta^n}{\partial x} - E^{(i)}_{j\xi\xi}\frac{\partial \zeta^n}{\partial y} + F^{(r)}_{j\xi\xi}\frac{\partial \xi^n}{\partial x} + \tau^w_x D^{(r)}_{j\xi\xi} - \tau^w_y D^{(i)}_{j\xi\xi}\right]\frac{\partial \xi^n}{\partial x} \\ & + \left[E^{(i)}_{j\xi\xi}\frac{\partial \zeta^n}{\partial x} + E^{(r)}_{j\xi\xi}\frac{\partial \zeta^n}{\partial y} + F^{(r)}_{j\xi\xi}\frac{\partial \xi^n}{\partial y} + \tau^w_x D^{(i)}_{j\xi\xi} + \tau^w_y D^{(r)}_{j\xi\xi}\right]\frac{\partial \xi^n}{\partial y} \\ & + \left[F^{(r)}_{jh\xi}\frac{\partial h}{\partial x} + F^{(r)}_{jh\xi}\frac{\partial h}{\partial y}\right]\frac{\partial \xi^n}{\partial x} + \left[F^{(r)}_{jh\xi}\frac{\partial h}{\partial y} - F^{(i)}_{jh\xi}\frac{\partial h}{\partial x}\right]\frac{\partial \xi^n}{\partial y} \\ & + \left[E^{(i)}_{jh\xi}\frac{\partial h}{\partial x} - E^{(r)}_{jh\xi}\frac{\partial h}{\partial y}\right]\frac{\partial \zeta^n}{\partial x} + \left[E^{(r)}_{jh\xi}\frac{\partial h}{\partial y} - E^{(i)}_{jh\xi}\frac{\partial h}{\partial x}\right]\frac{\partial \zeta^n}{\partial y} \\ & + \tau^w_x\left[D^{(r)}_{jh\xi}\frac{\partial h}{\partial x} + D^{(i)}_{jh\xi}\frac{\partial h}{\partial y}\right] + \tau^w_y\left[D^{(r)}_{jh\xi}\frac{\partial h}{\partial y} - D^{(i)}_{jh\xi}\frac{\partial h}{\partial x}\right] \end{aligned}$$

$$G_{6j} = F_{j\xi}^{(r)}\left[\left(\frac{\partial \xi^n}{\partial x}\right)^2 + \left(\frac{\partial \xi^n}{\partial y}\right)^2\right] + \left[E_{j\xi}^{(r)}\frac{\partial \xi^n}{\partial x} + E_{j\xi}^{(i)}\frac{\partial \xi}{\partial y}\right]\frac{\partial \zeta^n}{\partial x} + \left[E_{j\xi}^{(r)}\frac{\partial \xi}{\partial y} - E_{j\xi}^{(i)}\frac{\partial \xi}{\partial x}\right]\frac{\partial \zeta^n}{\partial y}$$

$$- \tau_x^w\left[D_{jh}^{(r)}\frac{\partial h}{\partial x} + D_{jh}^{(i)}\frac{\partial h}{\partial y}\right] + \tau_y^w\left[D_{jh}^{(i)}\frac{\partial h}{\partial x} - D_{jh}^{(r)}\frac{\partial h}{\partial y}\right] + G_{5j}\xi_{k,\,l}^n$$

where

$$E_{j\xi\xi}^{(r)} = \frac{\partial^2 E_j^{(r)}}{\partial \xi^2},\quad E_{jh\xi}^{(r)} = \frac{\partial^2 E_j^{(r)}}{\partial h\,\partial \xi},\quad \ldots$$

and

$$\frac{\partial \xi^n}{\partial x} = \frac{\xi_{k+1,\,l}^n - \xi_{k-1,\,l}^{n+1}}{2\Delta}$$

$$\frac{\partial \xi^n}{\partial y} = \frac{\xi_{k,\,l+1}^n - \xi_{k,\,l-1}^{n+1}}{2\Delta}$$

$$\nabla^2\xi^n = \frac{\xi_{k+1,\,l}^n + \xi_{k-1,\,l}^{n+1} + \xi_{k,\,l+1}^n + \xi_{k,\,l-1}^{n+1} - 4\xi_{k,\,l}^n}{\Delta^2}$$

The $\partial\zeta^n/\partial x$, $\partial\zeta^n/\partial y$, and $\nabla^2\zeta^n$ difference equations are the same as for ξ.

$$G_{7j} = \tau_x^w D_{j\xi}^{(r)} - \tau_y^w D_{j\xi}^{(i)} + E_{j\xi}^{(r)}\frac{\partial \zeta^n}{\partial x} - E_{j\xi}^{(i)}\frac{\partial \zeta^n}{\partial y} + F_{j\xi}^{(r)}\frac{\partial \xi^n}{\partial x} - F_{j\xi}^{(i)}\frac{\partial \xi^n}{\partial y}$$

$$G_{8j} = -\tau_x^w D_j^{(r)} + \tau_y^w D_j^{(i)} + G_{7j}\xi_{k,\,l}^n$$

$$G_{9j} = \tau_x^w D_{j\xi}^{(i)} + \tau_y^w D_{j\xi}^{(r)} + E_{j\xi}^{(r)}\frac{\partial \zeta^n}{\partial y} + E_{j\xi}^{(i)}\frac{\partial \zeta^n}{\partial x} + F_{j\xi}^{(r)}\frac{\partial \xi^n}{\partial y} + F_{j\xi}^{(i)}\frac{\partial \xi^n}{\partial x}$$

$$G_{10j} = -\tau_x^w D_j^{(i)} - \tau_y^w D_j^{(r)} + G_{9j}\xi_{k,\,l}^n$$

$$E_{1\xi} = \frac{\partial E_1}{\partial \xi} = -2i\alpha_1 + 2i\kappa_\tau \left\{ \Delta\rho\ \rho_r DSCK + \frac{2\rho_r e^{-a_2}}{K} \left[-\left(\frac{C_K}{K} + \alpha_2 \right) \left(e^{2a_1} - 1 \right) + 2\alpha_1 e^{2a_1} \right] \right\}$$

$$DSCK = \frac{1}{\omega} \frac{\partial}{\partial \xi} \left[\frac{\left(e^{2a_1} - 1 \right) \left(1 + e^{-2a_2} \right)}{K} \right]$$

$$DCCK = \frac{1}{K} \left[2\alpha_1 e^{2a_1} \left(1 + e^{-2a_2} \right) - 2\alpha_2 e^{-2a_2} \left(e^{2a_1} - 1 \right) - \frac{C_K}{K} \left(e^{2a_1} - 1 \right) \left(1 + e^{-2a_2} \right) \right]$$

$$F_{1\xi} = E_{1\xi} + 2i\alpha_1 - 2i\kappa_\tau DSCK$$

$$D_{2\xi} = -\frac{\omega D_2 C_K}{K} - \frac{4e^{a_1}}{K\omega} \left[e^{-a_2} (\alpha_1 - \alpha_2) + e^{-2a_2} \left(\alpha_2 - \frac{1}{2} \alpha_1 \right) - \frac{1}{2} \alpha_1 \right]$$

$$E_{2\xi} = -\frac{E_2 \omega C_K}{K} + \frac{2i}{K} \left(2\rho_r \Delta\rho \left\{ 2\alpha_1 e^{2a_1} \left[e^{-a_2} - \frac{1}{2} \left(1 + e^{-2a_2} \right) \right] \right. \right.$$

$$\left. + \alpha_2 \left(-e^{-a_2} + e^{-2a_2} \right) \left(e^{2a_1} - 1 \right) \right\} + \rho_r \left\{ \alpha_2 K + (a_2 + 1) C_K \right.$$

$$\left. \left. + 2e^{-a_2} \left[\alpha_2 \left(e^{2a_1} - 1 \right) - 2\alpha_1 e^{2a_1} \right] - 4.0\ \alpha_1 e^{2a_1} (\kappa_\tau - 1) \right\} \right)$$

$$F_{2\xi} = E_{2\xi} - \omega (F_2 - E_2) \frac{C_K}{K} - \frac{4i}{K} \left\{ \alpha_2 \left(e^{2a_1} - 1 \right) \left(-e^{-a_2} + e^{-2a_2} \right) \right.$$

$$\left. + 2\alpha_1 e^{2a_1} \left[e^{-a_2} - \frac{1}{2} \left(1 + e^{-2a_2} \right) \right] \right\}$$

$$D_{1h} = \frac{\alpha_2}{K\omega} \left[4\kappa_\tau e^{a_1} e^{-2a_2} - K_h \left(\frac{iD_1}{2} - 1 \right) \right]$$

$$K_h = -2e^{-2a_2}\left[\kappa_\tau\left(1 + e^{2a_1}\right) + \left(e^{2a_1} - 1\right)\right] = \frac{1}{\alpha_2\omega}\frac{\partial K}{\partial h}$$

$$E_{1h} = -\frac{K_h\omega\alpha_2}{K}(E_1 + 2i\alpha_1\xi) + \frac{4i\kappa_\tau\alpha_2}{K}\left[\left(e^{2a_1} - 1\right)\left(-\rho_r\,\Delta\rho\, e^{-2a_2} - \rho_r e^{-a_2}\right)\right]$$

$$F_{1h} = E_{1h} + \frac{2i\alpha_2\kappa_\tau\left(e^{2a_1} - 1\right)}{K}\left[2e^{-2a_2} + \frac{K_h}{h}\left(1 + e^{-2a_2}\right)\right]$$

$$D_{2h} = -\frac{\alpha_2}{K}\left[D_2K_h\omega + \frac{4}{\omega}\left(-e^{-a_2} + e^{-2a_2}\right)e^{a_1}\right]$$

$$E_{2h} = \frac{\alpha_2}{K}\left\{-K_h\omega E_2 + 2i\rho_r\left[2e^{-a_2}\left(e^{2a_1} - 1\right) + K_h(a_2 + 1) + K\right]\right.$$

$$\left. + 4i\rho_r\,\Delta\rho\left(-e^{-a_2} + e^{-2a_2}\right)\left(e^{2a_1} - 1\right)\right\}$$

$$F_{2h} = E_{2h} - \alpha_2(F_2 - E_2)\frac{K_h}{K}\omega - \frac{4i\alpha_2}{K}\left(e^{-2a_2} - e^{-a_2}\right)\left(e^{2a_1} - 1\right)$$

APPENDIX B

COEFFICIENTS FOR THE DIFFERENCE EQUATIONS

In this appendix the coefficients D_j, E_j, F_j, and their derivatives are all evaluated at $\xi^n_{k,\ell}$ and the local h value.

$$G_{1j} = E^{(r)}_{j\xi}\frac{\partial \zeta^n}{\partial x} - E^{(i)}_{j\xi}\frac{\partial \zeta^n}{\partial y} + 2F^{(r)}_{j\xi}\frac{\partial \xi^n}{\partial x} + \tau^w_x D^{(r)}_{j\xi} - \tau^w_y D^{(i)}_{j\xi} + F^{(r)}_{jh}\frac{\partial h}{\partial x} + F^{(i)}_{jh}\frac{\partial h}{\partial y}$$

$$G_{2j} = E^{(i)}_{j\xi}\frac{\partial \zeta^n}{\partial x} + E^{(r)}_{j\xi}\frac{\partial \zeta^n}{\partial y} + 2F^{(r)}_{j\xi}\frac{\partial \xi^n}{\partial y} + \tau^w_x D^{(i)}_{j\xi} + \tau^w_y D^{(r)}_{j\xi} + F^{(r)}_{jh}\frac{\partial h}{\partial y} - F^{(i)}_{jh}\frac{\partial h}{\partial x}$$

$$G_{3j} = E^{(r)}_{j\xi}\frac{\partial \xi^n}{\partial x} + E^{(i)}_{j\xi}\frac{\partial \xi^n}{\partial y} + E^{(r)}_{jh}\frac{\partial h}{\partial x} + E^{(i)}_{jh}\frac{\partial h}{\partial y}$$

$$G_{4j} = E^{(r)}_{j\xi}\frac{\partial \xi^n}{\partial y} - E^{(i)}_{j\xi}\frac{\partial \xi^n}{\partial x} + E^{(r)}_{jh}\frac{\partial h}{\partial y} - E^{(i)}_{jh}\frac{\partial h}{\partial x}$$

$$\begin{aligned} G_{5j} = {} & F^{(r)}_{j\xi}\nabla^2\xi^n + E^{(r)}_{j\xi}\nabla^2\zeta^n + \left[E^{(r)}_{j\xi\xi}\frac{\partial \zeta^n}{\partial x} - E^{(i)}_{j\xi\xi}\frac{\partial \zeta^n}{\partial y} + F^{(r)}_{j\xi\xi}\frac{\partial \xi^n}{\partial x} + \tau^w_x D^{(r)}_{j\xi\xi} - \tau^w_y D^{(i)}_{j\xi\xi}\right]\frac{\partial \xi^n}{\partial x} \\ & + \left[E^{(i)}_{j\xi\xi}\frac{\partial \zeta^n}{\partial x} + E^{(r)}_{j\xi\xi}\frac{\partial \zeta^n}{\partial y} + F^{(r)}_{j\xi\xi}\frac{\partial \xi^n}{\partial y} + \tau^w_x D^{(i)}_{j\xi\xi} + \tau^w_y D^{(r)}_{j\xi\xi}\right]\frac{\partial \xi^n}{\partial y} \\ & + \left[F^{(r)}_{jh\xi}\frac{\partial h}{\partial x} + F^{(r)}_{jh\xi}\frac{\partial h}{\partial y}\right]\frac{\partial \xi^n}{\partial x} + \left[F^{(r)}_{jh\xi}\frac{\partial h}{\partial y} - F^{(i)}_{jh\xi}\frac{\partial h}{\partial x}\right]\frac{\partial \xi^n}{\partial y} \\ & + \left[E^{(i)}_{jh\xi}\frac{\partial h}{\partial x} - E^{(r)}_{jh\xi}\frac{\partial h}{\partial y}\right]\frac{\partial \zeta^n}{\partial x} + \left[E^{(r)}_{jh\xi}\frac{\partial h}{\partial y} - E^{(i)}_{jh\xi}\frac{\partial h}{\partial x}\right]\frac{\partial \zeta^n}{\partial y} \\ & + \tau^w_x\left[D^{(r)}_{jh\xi}\frac{\partial h}{\partial x} + D^{(i)}_{jh\xi}\frac{\partial h}{\partial y}\right] + \tau^w_y\left[D^{(r)}_{jh\xi}\frac{\partial h}{\partial y} - D^{(i)}_{jh\xi}\frac{\partial h}{\partial x}\right] \end{aligned}$$

$$G_{6j} = F_{j\xi}^{(r)}\left[\left(\frac{\partial \xi^n}{\partial x}\right)^2 + \left(\frac{\partial \xi^n}{\partial y}\right)^2\right] + \left[E_{j\xi}^{(r)}\frac{\partial \xi^n}{\partial x} + E_{j\xi}^{(i)}\frac{\partial \xi}{\partial y}\right]\frac{\partial \zeta^n}{\partial x} + \left[E_{j\xi}^{(r)}\frac{\partial \xi}{\partial y} - E_{j\xi}^{(i)}\frac{\partial \xi}{\partial x}\right]\frac{\partial \zeta^n}{\partial y}$$

$$- \tau_x^w\left[D_{jh}^{(r)}\frac{\partial h}{\partial x} + D_{jh}^{(i)}\frac{\partial h}{\partial y}\right] + \tau_y^w\left[D_{jh}^{(i)}\frac{\partial h}{\partial x} - D_{jh}^{(r)}\frac{\partial h}{\partial y}\right] + G_{5j}\xi_{k,\,l}^n$$

where

$$E_{j\xi\xi}^{(r)} = \frac{\partial^2 E_j^{(r)}}{\partial \xi^2}, \quad E_{jh\xi}^{(r)} = \frac{\partial^2 E_j^{(r)}}{\partial h\, \partial \xi}, \quad \ldots$$

and

$$\frac{\partial \xi^n}{\partial x} = \frac{\xi_{k+1,\,l}^n - \xi_{k-1,\,l}^{n+1}}{2\Delta}$$

$$\frac{\partial \xi^n}{\partial y} = \frac{\xi_{k,\,l+1}^n - \xi_{k,\,l-1}^{n+1}}{2\Delta}$$

$$\nabla^2 \xi^n = \frac{\xi_{k+1,\,l}^n + \xi_{k-1,\,l}^{n+1} + \xi_{k,\,l+1}^n + \xi_{k,\,l-1}^{n+1} - 4\xi_{k,\,l}^n}{\Delta^2}$$

The $\partial \zeta^n/\partial x$, $\partial \zeta^n/\partial y$, and $\nabla^2 \zeta^n$ difference equations are the same as for ξ.

$$G_{7j} = \tau_x^w D_{j\xi}^{(r)} - \tau_y^w D_{j\xi}^{(i)} + E_{j\xi}^{(r)}\frac{\partial \zeta^n}{\partial x} - E_{j\xi}^{(i)}\frac{\partial \zeta^n}{\partial y} + F_{j\xi}^{(r)}\frac{\partial \xi^n}{\partial x} - F_{j\xi}^{(i)}\frac{\partial \xi^n}{\partial y}$$

$$G_{8j} = - \tau_x^w D_j^{(r)} + \tau_y^w D_j^{(i)} + G_{7j}\xi_{k,\,l}^n$$

$$G_{9j} = \tau_x^w D_{j\xi}^{(i)} + \tau_y^w D_{j\xi}^{(r)} + E_{j\xi}^{(r)}\frac{\partial \zeta^n}{\partial y} + E_{j\xi}^{(i)}\frac{\partial \zeta^n}{\partial x} + F_{j\xi}^{(r)}\frac{\partial \xi^n}{\partial y} + F_{j\xi}^{(i)}\frac{\partial \xi^n}{\partial x}$$

$$G_{10j} = - \tau_x^w D_j^{(i)} - \tau_y^w D_j^{(r)} + G_{9j}\xi_{k,\,l}^n$$

REFERENCES

1. Sundaram, T. R.; Easterbrook, C. C.; Piech, K. R.; and Rudinger, G.: An Investigation of the Physical Effects of Thermal Discharges into Cayuga Lake. Rep. CAL-VT-2616-0-2, Cornell Aeronautical Laboratory, Inc. Nov. 1969.

2. Hutchinson, G. E.: A Treatise on Limnology. Vol. 1. John Wiley & Sons, Inc., 1957.

3. Welander, P.: Wind-Driven Circulation in One- and Two-Layer Oceans of Variable Depth. Tellus, vol. 20, no. 1, 1968, pp. 1-15.

4. Hamblin, P. F.: Hydraulic and Wind-Induced Circulation in a Model of a Great Lake. Proceedings of the 12th Conferenceon Great Lakes Research. International Association of Great Lakes Research, 1969, pp. 567-582.

5. Welander, P.: Wind Action on a Shallow Sea: Some Generalizations of Ekman's Theory. Tellus, vol. 9, no. 1, Feb. 1957, pp. 45-52.

6. Gedney, Richard T.; and Lick Wilbert: Numerical Calculations of the Wind-Driven Currents in Lake Erie and Comparison with Measurements. Presented at the 14th Great Lakes Research Conference, Toronto, Ont., Apr. 19, 1971.

7. Lee, K. K.: Wind Induced Circulation in a Two-Layer Stratified Basin. Ph.D. Thesis, Cornell University, 1969.

8. Gedney, Richard T.: Numerical Calculations of the Wind-Driven Currents in Lake Erie. Ph.D. Thesis, Case Western Reserve Univ., 1971.

9. Gedney, R. T.; and Lick, W.: Wind-Driven Currents in Lake Erie. Geophys. Res., vol. 77, no. 10, Apr. 1972.

10. Wilson, Basil W.: Note on Surface Wind Stress over Water at Low and High Wind Speeds. J. Geophys. Res., vol. 65, no. 10, Oct. 1960, pp. 3377-3382.

11. Federal Water Quality Administration: Lake Erie Environmental Summary, 1963-1964. United States Department of Interior, May 1968.

NASA-Langley, 1972 —— 12 E-6776